

Fast Sample Size Determination for Bayesian Equivalence Tests

Luke Hagar* Nathaniel T. Stevens

*Department of Statistics & Actuarial Science
University of Waterloo, Waterloo, ON, Canada, N2L 3G1*

Abstract

Equivalence testing allows one to conclude that two characteristics are practically equivalent. We propose a framework for fast sample size determination with Bayesian equivalence tests facilitated via posterior probabilities. We assume that data are generated using statistical models with fixed parameters for the purposes of sample size determination. Our framework leverages an interval-based approach, which defines a distribution for the sample size to control the length of posterior highest density intervals (HDIs). We prove the normality of the limiting distribution for the sample size, and we consider the relationship between posterior HDI length and the statistical power of Bayesian equivalence tests. We introduce two novel approaches for estimating the distribution for the sample size, both of which are calibrated to align with targets for statistical power. Both approaches are much faster than traditional power calculations for Bayesian equivalence tests. Moreover, our method requires users to make fewer choices than traditional simulation-based methods for Bayesian sample size determination. It is therefore more accessible to users accustomed to frequentist methods.

Keywords: Bayesian power analysis; design and analysis of experiments; interval-based sample size determination; practical equivalence; the Bernstein-von Mises theorem; two-group comparisons

1 Introduction

1.1 Two-Group Equivalence Tests

Equivalence testing (Spiegelhalter et al., 1994; Wellek, 2010; Walker and Nowacki, 2011; Anderson-Cook and Borror, 2016) allows practitioners to account for practical equivalence when comparing two scalar quantities θ_1 and θ_2 . In this context, θ_j is a characteristic that describes group $j = 1, 2$ with $j = 1$ commonly representing the reference group. These comparisons are typically facilitated using the difference between the characteristics: $\theta_1 - \theta_2$. Equivalence testing defines an equivalence margin $\delta > 0$, which is the smallest difference between θ_1 and θ_2 that is of practical importance. The corresponding interval $(-\delta, \delta)$ is a region of practical equivalence (ROPE) that reflects a continuum of differences that are small enough to be considered practically negligible.

Several Bayesian methods for equivalence testing exist, including approaches with Bayes factors, credible intervals, and posterior probabilities. Morey and Rouder (2011) proposed the nonoverlapping hypotheses approach, which uses Bayes factors to compare the complementary hypotheses $H_0 : \theta_1 - \theta_2 \in (-\delta, \delta)$ and $H_1 : \theta_1 - \theta_2 \notin (-\delta, \delta)$. Kruschke (2018) proposed a method that facilitates equivalence testing using highest density intervals (HDIs). This method is called the HDI + ROPE decision rule (Kruschke, 2011, 2013), and

*Luke Hagar is the corresponding author and may be contacted at lmhagar@uwaterloo.ca.

it compares the ROPE $(-\delta, \delta)$ to the 95% HDI of the posterior for $\theta_1 - \theta_2$. Depending on whether the 95% HDI lies entirely within the ROPE, entirely outside the ROPE, or partially overlaps the ROPE, one should respectively conclude that the two groups are practically equivalent, conclude practical inequivalence, or refrain from drawing a conclusion.

Equivalence testing methods with posterior probabilities have been introduced in a variety of settings (see e.g., Spiegelhalter et al. (2004); Berry et al. (2011); Brutti et al. (2014); Makowski et al. (2019)). In a broader context that encompasses equivalence testing, Stevens and Hagar (2022) proposed using posterior probabilities referred to as comparative probability metrics (CPMs) as a flexible and intuitive means of making two-group comparisons. Given data observed from two groups, the CPM is the following posterior probability:

$$CPM = Pr(\delta_1 < \theta_1 - \theta_2 < \delta_2 \mid data), \quad (1)$$

where the interval endpoints δ_1 and δ_2 are values specified by the user to account for practicality. Equivalence testing can be facilitated via a particular CPM called the probability of agreement (PoA) (Stevens et al., 2017, 2020). The PoA takes (δ_1, δ_2) to be the ROPE. Conclusions concerning whether $\theta_1 - \theta_2 \in (-\delta, \delta)$ are drawn using a conviction threshold $0.5 \leq \gamma < 1$. Depending on whether the PoA is greater than γ , less than $1 - \gamma$, or between $1 - \gamma$ and γ , one should respectively conclude that there is agreement between the two groups, conclude disagreement, or refrain from drawing a conclusion. Larger values of γ allow one to draw conclusions with more conviction. The equivalence testing framework also encompasses the notion of noninferiority. Appropriate choices for δ_1 and δ_2 in (1) facilitate noninferiority testing. Assuming larger values of θ_j are preferred, the intervals $(\delta_1, \delta_2) = (-\delta, \infty)$ and $(\delta_1, \delta_2) = (-\infty, \delta)$ prompt the probability of noninferiority (PoNI) with reference to groups 1 and 2, respectively.

Most equivalence tests involve difference-based comparisons. However, because human perception of the number line is likely nonlinear (Dehaene, 2003; Kemp et al., 2021), ratio-based comparisons may be easier to conceptualize when the characteristics are extremely small or large. The framework from Stevens and Hagar (2022) can be extended to compare $\theta_1 > 0$ and $\theta_2 > 0$ using ratios. In this case, the posterior distribution of θ_2/θ_1 facilitates two-group comparisons via the percentage increase (or decrease) of the characteristic in the comparison distribution ($j = 2$) versus the reference distribution ($j = 1$). Given data observed from both groups, the relevant CPM is the posterior probability

$$CPM = Pr(\delta_1 < \theta_2/\theta_1 < \delta_2 \mid data). \quad (2)$$

For ratio-based comparisons, $\delta_* > 0$ denotes an extension of the equivalence margin that defines the ROPE: a continuum of values such that the ratio θ_2/θ_1 is not practically different from 1. The value chosen for δ_* defines the PoA by taking $\delta_1 = \delta_2^{-1} = (1 + \delta_*)^{-1}$; this interval is symmetric around 1 on the relative scale. The value for δ_* could be chosen such that a $100\delta_*$ % increase would be the smallest percentage

increase over the reference metric θ_1 that would be of practical importance. Assuming larger values of θ_j are preferred, choosing $(\delta_1, \delta_2) = (0, 1 + \delta_*)$ gives the probability that θ_1 is noninferior to θ_2 . Likewise, the interval $(\delta_1, \delta_2) = ((1 + \delta_*)^{-1}, \infty)$ yields the PoNI for θ_2 .

For the remainder of this paper, the term Bayesian equivalence testing is used to refer to equivalence and noninferiority tests that are facilitated via posterior probabilities. Such equivalence tests are the focus of this work. Bayesian equivalence testing requires that a substantial proportion of the posterior distribution for $\theta_1 - \theta_2$ or θ_2/θ_1 is contained within the appropriate ROPE to determine whether θ_1 and θ_2 are practically equivalent. To ensure the relevant posterior is precisely estimated, sample size determination is an important component of the design of Bayesian equivalence tests.

1.2 Bayesian Sample Size Determination

Many methods for Bayesian sample size determination exist, including decision theoretic and performance-based approaches. Decision theoretic approaches directly incorporate utility functions and select a sample size by maximizing expected utility (see e.g., [Raiffa et al. \(1961\)](#); [Lindley \(1997\)](#)). Performance-based approaches ([Wang and Gelfand, 2002](#); [Brutti et al., 2014](#)) do not directly incorporate utility functions and instead aim to control inference for a scalar parameter θ to a specified degree of error. While decision theoretic approaches offer a fully Bayesian approach to sample size determination, advocates for performance-based approaches argue that choosing adequate utility functions can present practical challenges ([Joseph and Wolfson, 1997](#)). Proponents of decision theoretic approaches ([Lindley, 1997](#)) have posited that performance-based approaches may not be coherent in the sense of [Savage \(1972\)](#). Neither approach has been widely accepted. Readers are directed to a special issue of *The Statistician* ([Adcock, 1997](#)) for a thorough comparison of decision theoretic and performance-based approaches.

This subsection provides a brief overview of performance-based approaches with power-based and interval-based criteria, which aim for pre-experimental probabilistic control over testing procedures and interval estimates for θ . In pre-experimental settings, the data have not been observed and are random variables. We therefore let $\mathbf{Y}^{(n)}$ represent data from a random sample of size n . For two-group comparisons, $\mathbf{Y}^{(n)}$ may consist of n observations from each group. To implement performance-based approaches, we must specify a sampling distribution for $\mathbf{Y}^{(n)}$. Typically, a *design* prior $p_D(\theta)$ ([De Santis, 2007](#); [Berry et al., 2011](#); [Gubbiotti and De Santis, 2011](#)) is defined to model uncertainty regarding θ in pre-experimental settings. Design priors are often informative and concentrated on θ values that are relevant to the objective of the study. For equivalence-based designs, $p_D(\theta)$ may be concentrated near the ROPE or one of its boundaries. The design prior is rarely the same prior used to analyze the observed data, often called the *analysis* prior. The design prior gives rise to the prior predictive distribution of $\mathbf{Y}^{(n)}$:

$$p(\mathbf{y}^{(n)}) = \int p(\mathbf{y}^{(n)}|\theta)p_D(\theta)d\theta.$$

The relevant performance criteria defined for the Bayesian inferential methods hold when the data are generated from this prior predictive distribution. The design and analysis priors are sometimes called the sampling and fitting priors, respectively (Wang and Gelfand, 2002; Sahu and Smith, 2006).

Gubbiotti and De Santis (2011) defined two methodologies for choosing the sampling distribution of $\mathbf{Y}^{(n)}$: the conditional and predictive approaches. The conditional approach fixes a *design value* θ_0 for the parameter of interest. The performance-based criteria are then based on the probability density or mass function $f(y; \theta_0)$. The conditional approach is typically used in frequentist sample size calculations. On the other hand, the predictive approach uses a (nondegenerate) design prior $p_D(\theta)$. The predictive approach is arguably more consistent with the Bayesian framework, so methods involving the conditional approach have been underdeveloped. However, there are advantages to using the conditional approach, which are discussed in this paper, that may outweigh its weaknesses for certain practitioners.

Power-based approaches to sample size determination for equivalence tests with posterior probabilities have been proposed in a variety of contexts (Berry et al., 2011; Gubbiotti and De Santis, 2011; Brutti et al., 2014). In these contexts, we aim to select a sample size n to ensure the probability that $CPM \geq \gamma$ is at least Γ :

$$\mathbb{E}(\mathbb{I}(Pr(\delta_1 < \theta < \delta_2 | \mathbf{Y}^{(n)}) \geq \gamma)) \geq \Gamma, \quad (3)$$

for some conviction threshold $\gamma \in [0.5, 1)$, target power $\Gamma \in (0, 1)$, and where $\mathbf{Y}^{(n)} \sim p(\mathbf{y}^{(n)})$. We note that $\mathbf{Y}^{(n)} \sim p(\mathbf{y}^{(n)})$ does not necessarily imply that $\delta_1 < \theta < \delta_2$ unless the design prior $p_D(\theta)$ imposes such a constraint; however, $p_D(\delta_1 < \theta < \delta_2)$ provides an upper bound for the attainable target power. For two-group comparisons, $\theta = h(\theta_1, \theta_2)$ for some function $h(\cdot)$. In this paper, $h(\theta_1, \theta_2) = \theta_1 - \theta_2$ and $h(\theta_1, \theta_2) = \theta_2/\theta_1$ are of interest. For equivalence or noninferiority tests, δ_1 and δ_2 could be appropriately chosen as the lower or upper limits of the ROPE. The plot of the quantity in (3) as a function of the sample size n is often called the power curve.

Minimum sample sizes that satisfy performance-based criteria can be found analytically in certain situations where conjugate priors are used (see e.g., Spiegelhalter et al. (1994); Joseph and Belisle (1997); Sahu and Smith (2006)). To support study design more generally, sample sizes that satisfy performance-based criteria can be found using simulation (Wang and Gelfand, 2002; De Santis, 2007; Berry et al., 2011). Most simulation-based procedures for sample size determination with design priors follow the same general process. First, a sample size n is selected. Second, a value $\tilde{\theta}$ is drawn from the design prior $p_D(\theta)$. Third, data $\tilde{\mathbf{y}}^{(n)}$ are generated according to the model $f(y; \tilde{\theta})$. Fourth, the posterior of θ given $\tilde{\mathbf{y}}^{(n)}$ is approximated to check if this posterior satisfies the performance-based criterion. This process is repeated many times to determine whether the performance-based criterion is satisfied on average or with a desired probability for the selected sample size n .

These simulation-based approaches to sample size determination are flexible but can be difficult to im-

plement. First, they can be very computationally intensive as we must approximate many posteriors for each sample size n that is considered. Moreover, the practitioner must choose the sample sizes that are explored, and guidance on choosing these sample sizes is limited. Wang and Gelfand (2002) recommended using bisection methods or grid searches to find a suitable sample size n . De Santis (2007) and Brutti et al. (2014) suggested plotting the performance criterion (e.g., power) for several values of n to choose a suitable sample size. Practitioners are likely to waste time exploring sample sizes n that are much too large or small to efficiently satisfy their performance-based criterion. This may not be an issue once suitable inputs for sample size calculations have been selected, but practitioners must specify several inputs when designing Bayesian equivalence tests – including the conviction threshold γ , ROPE, target power Γ , and design and analysis priors. Certain combinations of these inputs may yield unattainable sample sizes, but it is difficult to quickly discard these designs when using traditional simulation-based methods.

In Bayesian analyses, effects are precisely estimated when relevant posterior distributions are sufficiently narrow (see e.g., Kruschke and Liddell (2018)). The precision of the posterior is typically controlled via interval-based approaches that impose criteria on the length and coverage of the posterior’s credible intervals. As more data are collected from two groups that are truly practically equivalent, both the power to conclude that θ is in the ROPE should increase and the length of credible intervals with fixed coverage should decrease. However, formal exploration of the relationship between the power of Bayesian equivalence tests and the length of posterior credible intervals is limited.

One interval-based approach is the length probability criterion (LPC) (De Santis and Pacifico, 2004; Brutti et al., 2014) The LPC aims to precisely determine the posterior of θ by ensuring that the length of $100 \times (1 - \alpha)\%$ posterior HDI is at most l with probability at least $p \in (0, 1)$. We let $L_{1-\alpha}(\cdot)$ denote the length of the $100 \times (1 - \alpha)\%$ HDI. For fixed coverage $1 - \alpha$, the LPC selects the smallest sample size n such that

$$Pr(L_{1-\alpha}(\mathbf{Y}^{(n)}) \leq l) \geq p.$$

The LPC generalizes earlier work by Joseph and Belisle (1997), which sought to control the average length of posterior credible intervals.

Stevens and Hagar (2022) proposed an interval-based methodology for sample size determination to be used with Bayesian equivalence testing. This method recommends a sample size n for each group to ensure the relevant posterior of θ is sufficiently narrow using a construct called the sufficient sample size distribution (SSSD). The SSSD was defined so that its $100 \times p^{\text{th}}$ percentile is the smallest sample size n such that the resulting $100 \times (1 - \alpha)\%$ HDI will have length at most l with probability at least p . Moreover, we let $F_l(n)$ be the cumulative distribution function (CDF) of the SSSD for a target interval length l with fixed coverage $1 - \alpha$. The SSSD’s inverse CDF is defined such that $F_l^{-1}(p) := \inf\{n \in \mathbb{Z}^+ : F_l(n) \geq p\}$. When

$\mathbf{Y}^{(n)} \sim p(\mathbf{y}^{(n)})$, the SSSD satisfies

$$Pr(L_{1-\alpha}(\mathbf{Y}^{(F_i^{-1}(p))}) \leq l) \geq p.$$

Stevens and Hagar (2022) exclusively considered the conditional approach to specify the prior predictive distribution of $\mathbf{Y}^{(n)}$. The SSSD assigns a distribution to the LPC under the conditional approach. This was not done in previous work on the LPC, most of which explored predictive approaches.

The SSSD was observed to be approximately normal in a variety of situations via simulation (Stevens and Hagar, 2022). However, theoretical justification for the SSSD being approximately normal was not explored. Furthermore, conditions under which the SSSD exists and this approximate normality holds were not clearly defined. Also, the procedure to estimate the SSSD suggested in Stevens and Hagar (2022) is computationally prohibitive in many situations where conjugate priors do not exist. Moreover, the sample size determination procedure proposed in Stevens and Hagar (2022) was tailored to a conviction threshold of $\gamma = 0.5$, which was shown to yield good agreement-disagreement classification performance. However, this method for sample size determination should be extended to accommodate a general conviction threshold $0.5 \leq \gamma < 1$ because choosing $\gamma = 0.5$ may be inappropriate for many equivalence tests. In addition, the relationship between the SSSD and the power of equivalence tests under the conditional approach was not thoroughly investigated. Thus, there are still unsolved problems associated with SSSD-based sample size determination for Bayesian equivalence testing.

1.3 Contributions

The remainder of this article is structured as follows. In Section 2, we describe a food expenditure example for which CPMs are used to compare gamma tail probabilities. This example is referenced throughout the chapter to illustrate the proposed methods. In Section 3, we state the conditions under which the SSSD is approximately normal and prove this result as a theorem. In Section 4, we detail how to estimate the limiting form of the SSSD (which does not account for the prior distributions) and how to align this distribution with power-based criteria. We introduce an improved simulation-based approach for SSSD estimation that incorporates prior information in Section 5; we also describe how to use the SSSD to obtain an extremely fast local approximation to the power curve near the target power. In Section 6, we use simulation to make recommendations for choosing between the two SSSD estimation methods, and we explore how well our methods estimate the SSSD and locally approximate the power curve. We provide concluding remarks and a discussion of extensions to this work in Section 7.

2 Illustrative Example

2.1 Estimation of Posterior Probabilities

We assume that data y_{ij} , $i = 1, \dots, n_j$, $j = 1, 2$ have been collected from the two groups being compared. We assume that the data in each group are independent and identically distributed. We let θ_j be a characteristic that summarizes distribution $j = 1, 2$. For ratio-based comparisons, we require $\theta_j > 0$. We discuss several potential choices for θ_j below. For instance, θ_j could be the distribution's mean ($\theta_j = \mathbb{E}[y_{ij}]$), variance ($\theta_j = \text{Var}[y_{ij}]$), coefficient of variation ($\theta_j = \text{Var}[y_{ij}]^{1/2}/\mathbb{E}[y_{ij}]$), or p^{th} percentile ($\theta_j = F_j^{-1}(p)$), where $F_j(\cdot)$ is the CDF for distribution $j = 1, 2$. We could also compare tail probabilities for each distribution such that $\theta_j = \text{Pr}(y_{ij} > \kappa)$, where κ is a relevant scalar value from the support of distributions $j = 1, 2$.

Given the data $\mathbf{y}_j = (y_{1j}, y_{2j}, \dots, y_{n_j j})^T$ for each group ($j = 1, 2$) and the joint posterior $p(\theta_1, \theta_2 \mid \mathbf{y}_1, \mathbf{y}_2)$, the posterior probability may be calculated as

$$\iint_{\mathcal{R}} p(\theta_1, \theta_2 \mid \mathbf{y}_1, \mathbf{y}_2) d\theta_1 d\theta_2, \quad (4)$$

where \mathcal{R} is the region corresponding to $\delta_1 \leq \theta_1 - \theta_2 \leq \delta_2$ and $\delta_1 \leq \theta_2/\theta_1 \leq \delta_2$ for the CPMs in (1) and (2), respectively. The integral in (4) cannot be evaluated analytically for many of the θ_j specifications suggested above, so computational methods can be used to approximate the posterior $p(\theta_1, \theta_2 \mid \mathbf{y}_1, \mathbf{y}_2)$.

In this paper, we obtain an approximate sample from a relevant posterior distribution $p(\theta \mid \text{data})$ using the sampling-importance-resampling (SIR) algorithm (Rubin, 1987, 1988; Smith and Gelfand, 1992). In this setting, a sample can be generated from a continuous proposal distribution $c(\mathbf{x})$. However, we want to sample from a distribution $\tilde{b}(\mathbf{x})$ that is absolutely continuous with respect to $c(\mathbf{x})$. That is, $c(\mathbf{x}) = 0$ implies that $\tilde{b}(\mathbf{x}) = 0$ for all \mathbf{x} . We also require a function $b(\mathbf{x})$ such that $b(\mathbf{x}) \propto \tilde{b}(\mathbf{x})$. Given a sample $\mathbf{x}_1, \dots, \mathbf{x}_v$ from $c(\mathbf{x})$, we compute sampling weights $e_s = b(\mathbf{x}_s)/c(\mathbf{x}_s)$ for $s = 1, \dots, v$. We sample $\{\mathbf{x}_1^*, \dots, \mathbf{x}_v^*\}$ from the discrete distribution over $\{\mathbf{x}_1, \dots, \mathbf{x}_v\}$ with sampling weights proportional to e_s , $s = 1, \dots, v$. It follows that $\{\mathbf{x}_1^*, \dots, \mathbf{x}_v^*\}$ is approximately distributed according to $\tilde{b}(\mathbf{x})$ (Smith and Gelfand, 1992).

The quality of the approximate sample returned by the SIR algorithm depends on how much the proposal distribution $c(\mathbf{x})$ resembles $\tilde{b}(\mathbf{x})$. The approximate sample is typically of comparable quality to those obtained via Markov chain Monte Carlo (MCMC) methods given an appropriate choice for $c(\mathbf{x})$ and sufficiently large values for $v \gg \nu$. However, the SIR algorithm is usually much faster than MCMC methods. Therefore, we recommend using the SIR algorithm when we must approximate continuous posterior distributions. The SIR algorithm is not appropriate when the posterior of θ is not continuous. We argue that using continuous posteriors is consistent with the notion of *practical* equivalence. However, MCMC methods can be used if the relevant posterior is not continuous. Guidance for choosing $c(\mathbf{x})$ is provided as the SIR algorithm is applied throughout this paper. In this context, using the SIR algorithm generates draws $\theta_{1,1}^*, \theta_{1,2}^*, \dots, \theta_{1,\nu}^*$

and $\theta_{2,1}^*, \theta_{2,2}^*, \dots, \theta_{2,\nu}^*$. These draws can be used to estimate posterior quantities, including CPMs:

$$\frac{1}{\nu} \sum_{k=1}^{\nu} \mathbb{I}_{(\delta_1, \delta_2)}(h(\theta_{1,k}, \theta_{2,k})), \quad (5)$$

where $h(\theta_1, \theta_2) = \theta_1 - \theta_2$ and $h(\theta_1, \theta_2) = \theta_2/\theta_1$ for the CPMs defined in (1) and (2), respectively.

2.2 Illustrative Example Comparing Gamma Tail Probabilities

Mexico’s National Institute of Statistics, Geography, and Informatics conducts a biennial survey to monitor the behaviour of household income and expenses. This survey, referred to by its Spanish acronym ENIGH, also monitors sociodemographic characteristics. Here, we use data from the ENIGH 2020 survey (INEGI, 2021) to illustrate how CPMs facilitate equivalence testing. Each surveyed household was assigned a socioeconomic class: lower, lower-middle, upper-middle, and upper. We use data collected from the lower-middle income households (the most populous class) in the central Mexican state of Aguascalientes. We split these households into two groups based on the sex of the household’s main provider. Each household has a weighting factor ranging from 49 to 298. For this illustrative analysis, we divide each weighting factor by 75 and round to the nearest integer. We use this modified weighting factor to repeat the observation for each household in our data set. Our comparison of interest involves household food expenditure. We exclude the 0.41% of households that report zero quarterly expenditure on food to accommodate the gamma model’s strictly positive support.

After accounting for this weighting and applying the necessary exclusions, we have $n_1 = 1959$ and $n_2 = 759$ observations in the male ($j = 1$) and female ($j = 2$) provider groups, respectively. The datum y_{ij} collected for each household $i = 1, \dots, n_j$, $j = 1, 2$ is its quarterly expenditure on food per person measured in thousands of Mexican pesos (MXN \$1000). Figure 1 illustrates that a gamma model is appropriate for these data. For $j = 1$ and 2, we consider the tail probabilities $\theta_j = Pr(y_{ij} > 4.82)$. The threshold of $\kappa = 4.82$ is the median quarterly food expenditure per person (in MXN \$1000) for *upper* income households in Aguascalientes after accounting for weighting factors. Thus, we use the ratio θ_2/θ_1 to compare the probabilities that lower-middle income households with male and female providers spend at least as much on food per person as the typical upper income household. For concision, this example emphasizes ratio-based comparisons over difference-based ones. The observed proportions of households that spend at least \$4820 MXN on food per person are $\hat{\theta}_1 = 0.186$ and $\hat{\theta}_2 = 0.175$.

We assign uninformative GAMMA(2,0.1) priors to both the shape α_j and rate β_j parameters of the gamma model for group $j = 1, 2$. We let $\boldsymbol{\eta}_j = (\alpha_j, \beta_j)$ for $j = 1, 2$. The corresponding maximum likelihood estimates are $\hat{\boldsymbol{\eta}}_{1,n_1} = (2.55, 0.76)$ and $\hat{\boldsymbol{\eta}}_{2,n_2} = (2.30, 0.69)$, where the second subscript denotes the sample size. The posteriors of $\boldsymbol{\eta}_1$ and $\boldsymbol{\eta}_2$ are continuous, so we implement the SIR algorithm from Section 2.1 with $\nu = 10^6$ and $\nu = 10^5$ independently for each group. We select the following proposal distribution $c_j(\cdot)$ for each group: $N(\hat{\boldsymbol{\eta}}_{j,n_j}, 1.5 \times I^{-1}(\hat{\boldsymbol{\eta}}_{j,n_j})/n_j)$, where $I(\cdot)$ is the Fisher information for the gamma model. We

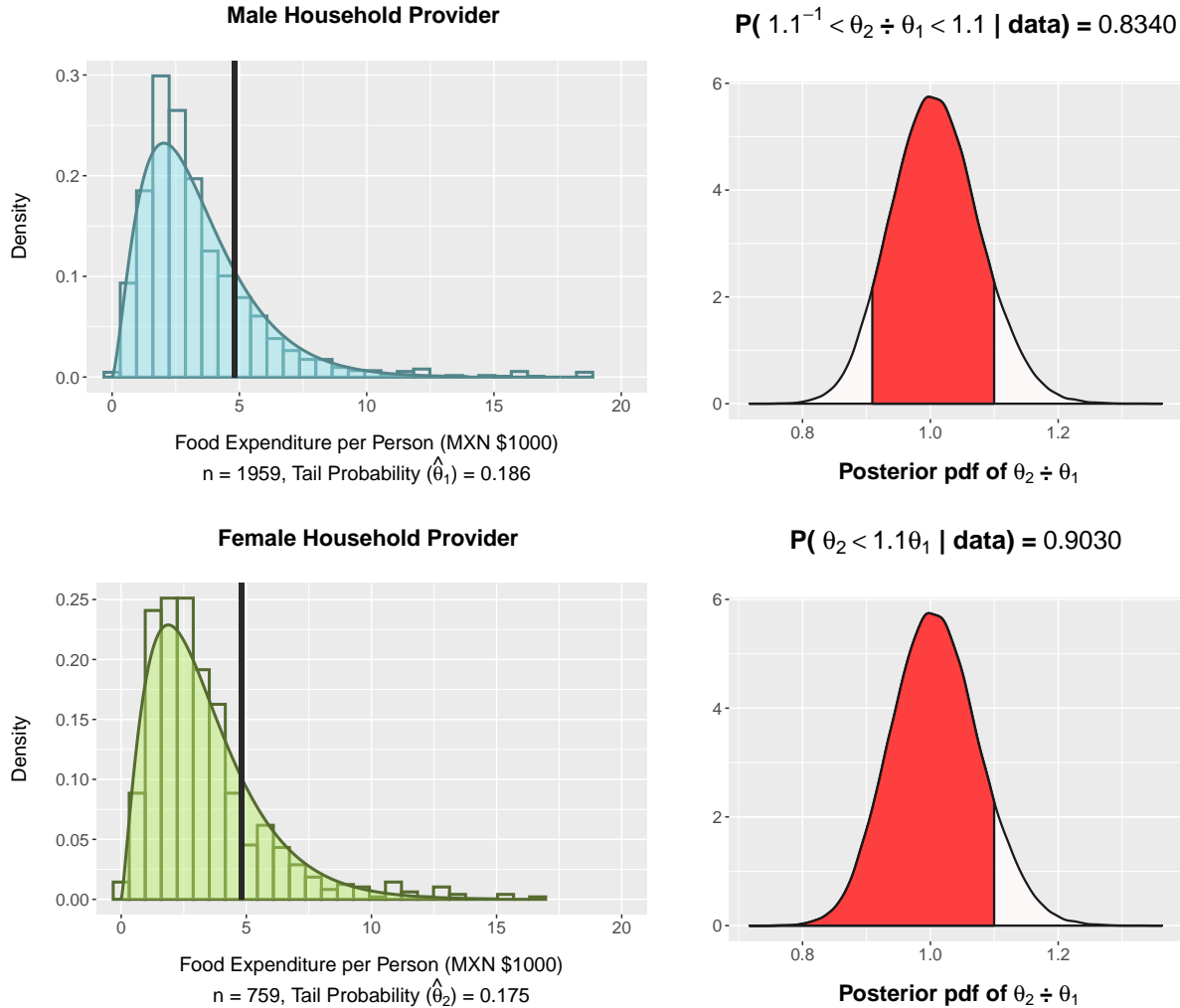


Figure 1: Group-specific summaries for quarterly food expenditure per person. Left: Food expenditure distributions. Right: Visualizations of the posterior and CPMs.

have inflated the variance of the approximately normal distribution for $\hat{\eta}_{j,n_j}$ (based only on the data) by 50% to ensure that observations from the tails of the true posterior for η_j (that incorporates prior information) are well represented in the sample from $c_j(\cdot)$, $j = 1, 2$. The $\nu = 10^5$ posterior draws for η_1 and η_2 can be used to compute draws from the posterior of θ_2/θ_1 . We also extract the posterior means for η_1 and η_2 . The gamma distributions characterized by these posterior means are superimposed on the histograms of the food expenditure data in Figure 1.

We now demonstrate how to compute posterior probabilities that facilitate equivalence testing. We first suppose that $\delta_* = 0.1$ for illustrative purposes. This implies that a 10% increase or decrease in the probability of spending at least as much on food per person as the typical upper income household is not of practical importance. Figure 1 illustrates that the PoA for this value of δ_* is 0.8340. We consider a conviction threshold of $\gamma = 0.9$. Because $0.1 < 0.8340 < 0.9$, we would refrain from drawing a conclusion

with respect to whether $\theta_2/\theta_1 \in (1.1^{-1}, 1.1)$. Figure 1 also displays the PoNI (0.9030). For $\gamma = 0.9$, this noninferiority test would indicate that households with male providers are, for practical purposes, at least as likely to spend $\geq \$4820$ MXN on food per person as those with female providers.

3 Theoretical Properties of the SSSD

3.1 Overview

The SSSD is defined such that when the sample size n is taken as its $100 \times p^{\text{th}}$ percentile, the resulting $100 \times (1 - \alpha)\%$ HDI will have length at most l with probability at least p (for a given l and α). We leverage the conditional approach, so this distribution assumes that data are generated from the selected response distributions parameterized by (fixed) user-specified design values. By using fixed parameters to generate the data, we do not account for uncertainty in the user’s guesses for the design values. However, using fixed parameter values is advantageous because it leads to the approximate normality of the SSSD, which has previously been conjectured via simulation (Stevens and Hagar, 2022).

To put forward a comprehensive framework for sample size determination with Bayesian equivalence testing, we provide theoretical justification for the approximate normality of the SSSD. This approximate normality is useful because it facilitates *fast* sample size determination, and its theoretical justification unifies the multiple components of our framework. In Section 3.2, we define the conditions under which the SSSD is approximately normal and state this result as a theorem. This theorem is proven in Section 3.3. In Section 3.4, we discuss practical considerations regarding the approximate normality and definition of the SSSD.

3.2 The Approximate Normality of the SSSD

The theoretical justification for the approximate normality of the SSSD relies on the Bernstein-von Mises (BvM) theorem (van der Vaart, 1998). Under certain conditions, the BvM theorem establishes the asymptotic equivalence between Bayesian credible sets of credibility level $1 - \alpha$ and confidence sets of confidence level $1 - \alpha$. We exploit this asymptotic equivalence between Bayesian and frequentist inference in our approach to sample size determination.

We assume that the underlying data generation process for the two groups of data is characterized by the models $f(y; \boldsymbol{\eta}_{1,0})$ and $f(y; \boldsymbol{\eta}_{2,0})$. Here, $f(\cdot)$ is the probability density or mass function selected for both groups of data, and $\boldsymbol{\eta}_{1,0}$ and $\boldsymbol{\eta}_{2,0}$ are fixed design value(s) for the distributional parameter(s). These distributions are herein referred to as *design* distributions. The design values $\boldsymbol{\eta}_{j,0}$ are different from the random variables $\boldsymbol{\eta}_j$ that parameterize the model for groups $j = 1, 2$ in Bayesian settings. To ensure that the SSSD is approximately normal, we also require that the models $f(y; \boldsymbol{\eta}_{1,0})$ and $f(y; \boldsymbol{\eta}_{2,0})$ satisfy the regularity conditions for the asymptotic normality of the maximum likelihood estimator (MLE) (Lehmann and Casella, 1998); these conditions include the independent and identically distributed assumption. When

specifying the models $f(y; \boldsymbol{\eta}_{j,0})$, we also specify fixed values $\theta_{j,0}$ for the random variables θ_j , $j = 1, 2$. These values are often specified implicitly as a function $g(\cdot)$ of the parameters $\boldsymbol{\eta}_{j,0}$: $\theta_{j,0} = g(\boldsymbol{\eta}_{j,0})$. We require that $g(\boldsymbol{\eta}_{j,0})$ is a differentiable with respect to $\boldsymbol{\eta}_{j,0}$ for $j = 1, 2$.

Theorem 1, which provides the necessary conditions for the approximate normality of the SSSD, is stated below. The conditions to invoke Theorem 1, including the conditions for the BvM theorem (van der Vaart, 1998) and the regularity conditions from Lehmann and Casella (1998), are detailed in Appendix A of the supplement (Hagar and Stevens, 2023). The approximate normality holds when the SSSD is defined for the posterior of a univariate parameter $\theta = h(\theta_1, \theta_2)$, where $h(\cdot)$ is a differentiable function with respect to θ_1 and θ_2 . Here, $h(\theta_1, \theta_2) = \theta_1 - \theta_2$ and $h(\theta_1, \theta_2) = \theta_2/\theta_1$ are of interest.

Theorem 1. *Let $f(y; \boldsymbol{\eta}_{1,0})$ and $f(y; \boldsymbol{\eta}_{2,0})$ satisfy the regularity conditions detailed in Lehmann and Casella (1998). Furthermore, let the prior for θ_j be continuous in a neighbourhood of $\theta_{j,0} = g(\boldsymbol{\eta}_{j,0})$ with positive density at $\theta_{j,0}$ for $j = 1, 2$. Let $F_l(n)$ be the SSSD's CDF for the target interval length l of the $100 \times (1 - \alpha)\%$ posterior HDI for $\theta = h(\theta_1, \theta_2)$, and let $\sigma_l = \sigma/l$. Then as $l \rightarrow 0^+$,*

$$\frac{F_l(n) - \mu_l}{\sigma_l} \xrightarrow{d} N(0, 1).$$

The proof of Theorem 1 is given in Section 3.3 along with the specifications for μ_l and $\sigma_l = \sigma/l$, where σ is a constant. We now briefly comment on the conditions required for the SSSD's approximate normality to hold as $l \rightarrow 0^+$. van der Vaart (1998) details four assumptions that must be satisfied in order to invoke the BvM theorem. The first three assumptions involve the models $f(y; \boldsymbol{\eta}_{1,0})$ and $f(y; \boldsymbol{\eta}_{2,0})$ and are weaker than the sufficient regularity conditions for the asymptotic normality of the MLE (Lehmann and Casella, 1998). Therefore, the first three assumptions for the BvM theorem are also necessarily satisfied in Theorem 1. These regularity conditions are satisfied for many probability distributions – including all members of the regular exponential family.

The final assumption regards prior specification for the random variables (van der Vaart, 1998). For our purposes, θ_1 and θ_2 are the random variables for which we explicitly or implicitly assign prior distributions. We require that the prior distribution of θ_j be continuous in a neighbourhood of $\theta_{j,0} = g(\boldsymbol{\eta}_{j,0})$ with positive density at $\theta_{j,0}$ for $j = 1, 2$. This final condition ensures that the posterior of $\theta = h(\theta_1, \theta_2)$ converges to a neighbourhood of $\theta_0 = h(\theta_{1,0}, \theta_{2,0})$. Alternative performance-based approaches to sample size determination (Joseph and Belisle, 1997; Wang and Gelfand, 2002; Brutti et al., 2014) are recommended when the conditions to invoke Theorem 1 are not satisfied.

3.3 Proof of Theorem 1

Under the conditions for Theorem 1, the BvM theorem states that the posterior of θ converges to a normal distribution with mean θ_0 and variance $I(\theta_0)^{-1}/n$ in the limit of infinite data (van der Vaart, 1998). Here,

$I(\theta_0)$ is the Fisher information for θ evaluated at the design value θ_0 . The length of the $100 \times (1 - \alpha)\%$ HDI is defined by this asymptotic variance: $I(\theta_0)^{-1}/n$. In practice, θ_0 is estimated from the to-be-observed data $\mathbf{Y}^{(n)}$ using the MLE $\hat{\theta}_n$. Given α and n , $L_{1-\alpha}(\mathbf{Y}^{(n)})$ can be estimated by

$$L_{1-\alpha}(\mathbf{Y}^{(n)}) = \frac{2z_{1-\alpha/2}}{\sqrt{n}} \times \sqrt{I(\hat{\theta}_n)^{-1}}, \quad (6)$$

where $z_{1-\alpha/2}$ is the $1 - \alpha/2$ quantile of the $N(0, 1)$ distribution. When the conditions for Theorem 1 hold, $L_{1-\alpha}(\mathbf{Y}^{(n)})$ is asymptotically normally distributed by the delta method. The mean of the SSSD μ_l is thus defined such that $\mathbb{E}(L_{1-\alpha}(\mathbf{Y}^{(\mu_l)})) = l$, where l is the target HDI length. When $n = \mu_l$, the asymptotic expectation of (6) gives

$$\mu_l = \frac{4z_{1-\alpha/2}^2 I(\theta_0)^{-1}}{l^2}. \quad (7)$$

We consider the probability p that $L_{1-\alpha}(\mathbf{Y}^{(n)}) \leq l$, yet the length criterion is either satisfied or not satisfied for a single posterior of θ . The binary nature of this information motivates us to consider the SSSD in the framework of binary regression. We consider a binary regression model with $l - L_{1-\alpha}(\mathbf{Y}^{(n)})$ as the latent variable and the sample size n as the single predictor. By (6), $\mathbb{E}(L_{1-\alpha}(\mathbf{Y}^{(n)}))$ is a function of $n^{-1/2}$. For large n , the relationship between $\mathbb{E}(L_{1-\alpha}(\mathbf{Y}^{(n)}))$ and n should be approximately linear for sample sizes that correspond to the probable domain of the SSSD. We note that as $l \rightarrow 0^+$, the samples sizes that correspond to the SSSD's probable domain increase in magnitude.

The error terms for $l - L_{1-\alpha}(\mathbf{Y}^{(n)})$ are approximately normal by the delta method, so a probit model could be appropriate. Let $W \in \{0, 1\}$ denote whether the length criterion is satisfied. We further let N be a random variable for the sample size. Conditional on the sample size, the approximate probit model would be given by

$$\Phi^{-1}(Pr(W = 1|N = n)) \approx \beta_0 + \beta_1 n, \quad (8)$$

where $W = 1$ if and only if $l - L_{1-\alpha}(\mathbf{Y}^{(n)}) \geq 0$ such that

$$l - L_{1-\alpha}(\mathbf{Y}^{(n)}) \approx \beta_0 + \beta_1 n + \varepsilon_n \text{ with } \varepsilon_n \sim N(0, 4z_{1-\alpha/2}^2 A^2/n^2), \quad (9)$$

where A^2 is the asymptotic variance of $\sqrt{n}(I(\hat{\theta}_n)^{-1/2} - I(\theta_0)^{-1/2})$. The error terms exhibit heteroscedasticity: $Var(L_{1-\alpha}(\mathbf{Y}^{(n)})) = 4z_{1-\alpha/2}^2 A^2/n^2$ decreases as n increases. The approximate probit model would be appropriate if the error terms were homoscedastic, and this result would lead to the approximate normality of the SSSD. For this reason, we show that this heteroscedasticity is negligible for large n . Theorem 1 states that the standard deviation of the SSSD $\sigma_l = \sigma/l$ involves a constant σ . For a given l , we can estimate σ_l if we know μ_l and which SSSD percentile another sample size n corresponds to. We call this estimate $\hat{\sigma}_{l,n}$

and can estimate $\hat{\sigma}_n = l \times \hat{\sigma}_{l,n}$ as

$$\begin{aligned}\hat{\sigma}_n &= l \times \frac{n - \mu_l}{\Phi^{-1}\left(\Phi\left(\frac{l - \mathbb{E}(L_{1-\alpha}(\mathbf{Y}^{(n)}))}{\sqrt{\text{Var}(L_{1-\alpha}(\mathbf{Y}^{(n)})}}\right)\right)} \\ &= 2z_{1-\alpha/2}A \times \frac{1 - \mu_l/n}{1 - \mathbb{E}(L_{1-\alpha}(\mathbf{Y}^{(n)}))/l}.\end{aligned}$$

By (6) and (7), we have that $\sqrt{n}\mathbb{E}(L_{1-\alpha}(\mathbf{Y}^{(n)})) = \sqrt{\mu_l}\mathbb{E}(L_{1-\alpha}(\mathbf{Y}^{(\mu_l)})) = \sqrt{\mu_l}l$. Equivalently, $\mathbb{E}(L_{1-\alpha}(\mathbf{Y}^{(n)})) = l \times \sqrt{\mu_l/n}$. Let $|a| < 3\sigma/l$. For $n = \mu_l + a$,

$$\hat{\sigma}_{\mu_l+a} = 2z_{1-\alpha/2}A \times \frac{1 - \frac{1}{1 + a/\mu_l}}{1 - \frac{1}{\sqrt{1 + a/\mu_l}}}.\quad (10)$$

The result from (7) implies that $\mu_l \rightarrow \infty$ as $l \rightarrow 0^+$. It follows that for arbitrary fixed a , $\lim_{l \rightarrow 0^+} \hat{\sigma}_{\mu_l+a} = 4z_{1-\alpha/2}A$ by (10) and L'Hôpital's rule. We let $\sigma = 4z_{1-\alpha/2}A$ and define the probable domain of the SSSD as $\{n \mid n \in (\mu_l \pm 3\sigma/l)\}$. For large sample sizes n , $\hat{\sigma}_n$ does not change drastically over the probable domain of the SSSD and so the impact of heteroscedasticity is not substantial. Thus, the approximate probit model from (8) and (9) is appropriate, and the SSSD is approximately normal.

3.4 Practical Implications of Theorem 1

We emphasize that $\mu_l = 4z_{1-\alpha/2}^2 I(\theta_0)^{-1}/l^2$ and $\sigma_l = 4z_{1-\alpha/2}A/l$ do not incorporate information from relevant prior distributions; they depend solely on the design distributions $f(y; \boldsymbol{\eta}_{1,0})$ and $f(y; \boldsymbol{\eta}_{2,0})$ and the choices for l and α . The design distributions impact both μ_l and σ_l via $I(\theta_0)^{-1}$ and A as defined in (9). The relationship between l and α also impacts μ_l and σ_l . For illustration, we let $z_{1-\alpha/2}/l = \tilde{c}$ for some constant $\tilde{c} > 0$. The values for the SSSD parameters from Theorem 1 simplify to $\mu_l = 4\tilde{c}^2 I(\theta_0)^{-1}$ and $\sigma_l = 4\tilde{c}A$. For given $f(y; \boldsymbol{\eta}_{1,0})$ and $f(y; \boldsymbol{\eta}_{2,0})$, all (α, l) pairs that yield $z_{1-\alpha/2}/l = \tilde{c}$ for a particular value of $\tilde{c} > 0$ have the same limiting form of the SSSD.

As $l \rightarrow 0^+$, both the lower and upper extremes of the SSSD's probable domain approach ∞ because μ_l and σ_l are functions of l^{-2} and l^{-1} , respectively. Moreover, these values for μ_l and σ_l can be used to determine percentiles of the SSSD. We formally state this result in Corollary 1, which follows from Theorem 1.

Corollary 1. *Let $\mu_l = 4z_{1-\alpha/2}^2 I(\theta_0)^{-1}/l^2$ and $\sigma_l = 4z_{1-\alpha/2}A/l$. If we obtain a sample of size $n = \mu_l + z_p\sigma_l$ from both $f(y; \boldsymbol{\eta}_{1,0})$ and $f(y; \boldsymbol{\eta}_{2,0})$, the probability that the $100 \times (1 - \alpha)\%$ posterior HDI for θ satisfies the length criterion approaches p as $l \rightarrow 0^+$.*

Strictly speaking, these values for μ_l and σ_l ensure that the $100 \times (1 - \alpha)\%$ confidence interval for θ has length at most l with probability at least p for fixed α . But because the BvM theorem establishes the asymptotic equivalence between $100 \times (1 - \alpha)\%$ credible and confidence intervals, we are ensured that the

$100 \times (1 - \alpha)\%$ HDI for the posterior of θ also has length at most l with probability at least p for reasonably large sample sizes (corresponding to small values of l). Similarly to how asymptotic normality is exploited for finite samples, we do not require that $l = 0$ to invoke Theorem 1. We explore the robustness of using these values for μ_l and σ_l to estimate the SSSD for nonzero values of l (and hence finite samples) via simulation in Section 6.

Lastly, we briefly comment on situations where the SSSD may be degenerate or ill defined. We note that informative prior distributions for $\theta_j, j = 1$ and 2 , often specified implicitly via the priors for $\boldsymbol{\eta}_j$, can present practical challenges when defining the SSSD for finite values of l . To illustrate this, we consider a (perhaps unrealistic) scenario where the length of the $100 \times (1 - \alpha)\%$ prior HDI for θ is less than the target length l . We first suppose that the priors for $\boldsymbol{\eta}_1$ and $\boldsymbol{\eta}_2$ have been well specified with respect to the design distributions. In this case, we never expect $L_{1-\alpha}(\mathbf{Y}^{(n)})$ to be greater than l . The SSSD is degenerate in this scenario. We note that the SSSD may also be degenerate for nonzero μ_l if the design distributions are specified such that A^2 , the asymptotic variance of $\sqrt{n}(I(\hat{\theta}_n)^{-1/2} - I(\theta_0)^{-1/2})$, is 0. We discuss this scenario in more detail in Appendix B.1 of the supplement.

We now suppose that the priors for $\boldsymbol{\eta}_1$ and $\boldsymbol{\eta}_2$ have been misspecified with respect to the design distributions but satisfy the assumptions for the BvM theorem. In this situation, the posterior of θ may first become more diffuse as the impact of the data $\mathbf{Y}^{(n)}$ overwhelms that of the misspecified priors. By the BvM theorem, the posterior of θ will eventually concentrate around the design value θ_0 . In these settings, it may be possible for $L_{1-\alpha}(\mathbf{Y}^{(n)})$ to have length at most l with probability approximately p for two sample sizes $n_{(1)} < n_{(2)}$. The SSSD is therefore not well defined in these scenarios.

The aforementioned scenarios are not of great concern because practitioners can readily determine whether the length criterion is satisfied a priori. Of more practical concern is the problematic behaviour that can occur for small sample sizes, particularly when uninformative priors are specified. For small sample sizes n , the posterior of θ may be volatile when uninformative priors are used. This can give rise to scenarios where $Pr(L_{1-\alpha}(\mathbf{Y}^{(n)}) \leq l)$ is not a nondecreasing function of n . Although small sample size scenarios are not the focus of this work, this phenomenon and its practical implications on sample size determination are briefly explored via simulation in Section 6.

We emphasize that problems with defining the SSSD cannot arise from selecting a small target length l that is unattainable. This follows by the BvM theorem because we assume that observations are generated independently and identically from the design distributions $f(y; \boldsymbol{\eta}_{1,0})$ and $f(y; \boldsymbol{\eta}_{2,0})$. This would not be true if we used the predictive approach to specify the sampling distribution of $\mathbf{Y}^{(n)}$. Problems with defining the SSSD are not of concern in the limiting case as $l \rightarrow 0^+$.

The following guidance can be used to alert practitioners to situations where the SSSD is degenerate or ill defined. Using informative priors typically decreases the length of the $100 \times (1 - \alpha)\%$ prior HDI for θ ,

but practitioners should ensure that this prior HDI length is still sufficiently larger than l . If uninformative priors are used and the SSSD’s probable domain includes small sample sizes, practitioners can use simulation to explore whether the SSSD is well defined. However, SSSD-based design is likely inappropriate for small sample size scenarios as Theorem 1 leverages asymptotic results. In these scenarios, the sample sizes near the lower extreme of the SSSD’s probable domain may even be negative, and alternative sample size determination methods should be used.

4 Aligning Interval-Based Criteria and Power

4.1 Choosing Targets for the HDI Length and Coverage

To use the SSSD for sample size determination, we must specify a target length l and coverage $1 - \alpha$ for the posterior HDI of θ . Stevens and Hagar (2022) recommended choosing α to be small and l to be equal to the length of the ROPE. This recommendation was tailored to a conviction threshold of $\gamma = 0.5$ and scenarios where the design value θ_0 is not too close to either δ_1 or δ_2 . Here, we provide more general guidance for selecting l and α that is applicable for a wider variety of equivalence tests.

Because we aim to draw a conclusion about whether $\theta \in (\delta_1, \delta_2)$ using a conviction threshold γ , we suggest selecting interval-based criteria that align with a target power Γ defined in (3). We aim for $100 \times \gamma\%$ of the posterior of θ to be contained in (δ_1, δ_2) . As such, it would be natural to work with $100 \times \gamma\%$ HDIs, and we recommend choosing $\alpha = 1 - \gamma$. It follows that the target length l should be less than $\delta_2 - \delta_1$: if we do not expect $100 \times (1 - \alpha)\%$ of the posterior to fall in any interval of length $\delta_2 - \delta_1$, then we cannot expect $100 \times \gamma\%$ of the posterior to be contained within the interval (δ_1, δ_2) . However, it is not clear how much smaller l should be than $\delta_2 - \delta_1$. If θ_0 is close to δ_1 or δ_2 , then l should likely be *substantially* smaller. Lastly, we note that the SSSD can also be used when l and α are not selected to align with power-based criteria.

In this section, we describe an approach to implicitly select a target length l based on a target power Γ , along with the design distributions and interval (δ_1, δ_2) . It should be more intuitive for practitioners to choose Γ than guess a value for $l < \delta_2 - \delta_1$. Aligning l with Γ requires some knowledge of the power curve, which can be computationally intensive to estimate. Our framework for sample size determination is interval-based. Yet, even practitioners who are interested in power-based criteria may prefer our methodology; the relationship between interval-based and power-based criteria can be used to approximate the power curve much faster than traditional methods. The remainder of this section sets a foundation for incorporating prior information into SSSD estimation and power curve approximation in Section 5. In Section 4.2, we develop a simulation-based procedure to quickly estimate the power curve that leverages the BvM theorem. We discuss how to align the target length l with this estimated power curve in Section 4.3. In Section 4.4, we demonstrate how to implement this approach.

4.2 Fast Approximation of the Power Curve

Traditional approaches to power curve estimation are slow for several reasons. First, we must simulate many samples from the design distributions to reliably estimate power for each value of n explored. Second, in the absence of conjugate priors, we must use computational methods to approximate the posterior corresponding to each generated sample. Third, we must choose which sample sizes n to explore, and we may waste time considering sample sizes that are much too large or small.

Because we aim to *roughly* estimate the power curve to select an appropriate HDI target length l , we develop an approach for power curve approximation that addresses these sources of computational inefficiency. For a given sample $\mathbf{y}^{(n)}$, we can compute maximum likelihood estimates $\hat{\boldsymbol{\eta}}_{1,n}$ and $\hat{\boldsymbol{\eta}}_{2,n}$, which yield an estimate for $\hat{\theta}_n$ via the functions $g(\cdot)$ and $h(\cdot)$. For sufficiently large n , the posterior of θ is approximately $N(\hat{\theta}_n, I(\hat{\theta}_n)^{-1}/n)$. We can quickly determine whether $100 \times \gamma\%$ of the $N(\hat{\theta}_n, I(\hat{\theta}_n)^{-1}/n)$ distribution is contained within the interval (δ_1, δ_2) . Given a representative sample of $\hat{\theta}_n$ values corresponding to samples from $f(y; \boldsymbol{\eta}_{1,0})$ and $f(y; \boldsymbol{\eta}_{2,0})$, the proportion of time that this occurs would roughly estimate power at the sample size n .

Given a sample size n , we do not simulate data $\mathbf{Y}^{(n)}$ from the prior predictive distribution. Instead, we simulate from the approximate distributions of the MLEs of $\boldsymbol{\eta}_1$ and $\boldsymbol{\eta}_2$. For sufficiently large n , the MLEs $\hat{\boldsymbol{\eta}}_{j,n}$ for groups $j = 1, 2$ approximately and independently follow $N(\boldsymbol{\eta}_{j,0}, I^{-1}(\boldsymbol{\eta}_{j,0})/n)$ distributions. We use low-discrepancy sequences and conditional probability distributions to obtain a sample of moderate size from the joint limiting distribution of $\hat{\boldsymbol{\eta}}_{1,n}$ and $\hat{\boldsymbol{\eta}}_{2,n}$, which has dimension $2d$. We use a Sobol' sequence $\mathbf{u}_1, \mathbf{u}_2, \dots, \mathbf{u}_{n_{sob}} \in [0, 1]^{2d}$ (Sobol', 1967) with length n_{sob} . Sobol' sequences are low-discrepancy sequences based on integer expansion in base 2. Appropriately randomized Sobol' sequences yield estimators with better consistency properties than those created using deterministic sequences, and this randomization can be appropriately carried out via a digital shift (Lemieux, 2009). We generate and randomize Sobol' sequences in R using the `qrng` package (Hofert and Lemieux, 2020). The dimension of the joint distribution of $\hat{\boldsymbol{\eta}}_{1,n}$ and $\hat{\boldsymbol{\eta}}_{2,n}$ is typically much smaller than $2n$, the dimension of the data $\mathbf{Y}^{(n)}$. It is therefore easier to obtain an efficient and representative sample from the joint distribution of $\hat{\boldsymbol{\eta}}_{1,n}$ and $\hat{\boldsymbol{\eta}}_{2,n}$ using low-discrepancy sampling methods.

Each draw $(\hat{\boldsymbol{\eta}}_{1,n}(\mathbf{u}_r), \hat{\boldsymbol{\eta}}_{2,n}(\mathbf{u}_r))$ from this joint limiting distribution depends solely on the design distributions and the Sobol' sequence draw \mathbf{u}_r , $r = 1, \dots, n_{sob}$. Both $\hat{\boldsymbol{\eta}}_{1,n}$ and $\hat{\boldsymbol{\eta}}_{2,n}$ are of dimension d . We use the notation $(\hat{\boldsymbol{\eta}}_{1,n}(\mathbf{u}_r), \hat{\boldsymbol{\eta}}_{2,n}(\mathbf{u}_r))$ but emphasize that $\hat{\boldsymbol{\eta}}_{1,n}(\mathbf{u}_r)$ and $\hat{\boldsymbol{\eta}}_{2,n}(\mathbf{u}_r)$ are functions of only the first and final d components of $\mathbf{u}_r \in [0, 1]^{2d}$, respectively. For each draw $(\hat{\boldsymbol{\eta}}_{1,n}(\mathbf{u}_r), \hat{\boldsymbol{\eta}}_{2,n}(\mathbf{u}_r))$, we consider the distributions $f(y; \hat{\boldsymbol{\eta}}_{1,n}(\mathbf{u}_r))$ and $f(y; \hat{\boldsymbol{\eta}}_{2,n}(\mathbf{u}_r))$. Upon computing these draws for a given value of n , we can treat $\boldsymbol{\eta}_{1,r} = \hat{\boldsymbol{\eta}}_{1,n}(\mathbf{u}_r)$ and $\boldsymbol{\eta}_{2,r} = \hat{\boldsymbol{\eta}}_{2,n}(\mathbf{u}_r)$ as fixed design values for $r = 1, \dots, n_{sob}$. This allows us to compute $\theta_{j,r} = g(\boldsymbol{\eta}_{j,r})$ for $j = 1, 2$, yielding $\theta_r = h(\theta_{1,r}, \theta_{2,r})$ and $I(\theta_r)^{-1}$. To find $I(\theta_0)^{-1}$, we find the

limiting distributions for $\sqrt{n}(\hat{\boldsymbol{\eta}}_{j,n} - \boldsymbol{\eta}_{j,0})$, $j = 1, 2$. We use the multivariate delta method to obtain the limiting distribution for $\sqrt{n}(\hat{\boldsymbol{\theta}}_n - \boldsymbol{\theta}_0)$, where $\hat{\boldsymbol{\theta}}_n$ is a function of $\hat{\boldsymbol{\eta}}_{1,n}$ and $\hat{\boldsymbol{\eta}}_{2,n}$. The inverse of the Fisher information $I(\boldsymbol{\theta}_0)^{-1}$ is the variance of the limiting distribution for $\sqrt{n}(\hat{\boldsymbol{\theta}}_n - \boldsymbol{\theta}_0)$. To instead find $I(\boldsymbol{\theta}_r)^{-1}$, we replace the fixed values $\boldsymbol{\theta}_0$, $\boldsymbol{\eta}_{1,0}$, and $\boldsymbol{\eta}_{2,0}$ with their counterparts determined by $\boldsymbol{\eta}_{1,r}$ and $\boldsymbol{\eta}_{2,r}$.

For $r = 1, \dots, n_{sob}$, we consider the limiting posterior imposed by the BvM theorem: $N(\boldsymbol{\theta}_r, I(\boldsymbol{\theta}_r)^{-1}/n)$. We then determine whether $100 \times \gamma\%$ of this normal distribution is contained within the interval (δ_1, δ_2) for $r = 1, \dots, n_{sob}$. The proportion of the n_{sob} times that this occurs roughly estimates the value of the power curve at n . If we repeat this process for several appropriate values of n , we can roughly approximate the entire power curve. Unfortunately, such a process would still require users to choose appropriate sample sizes n , limiting its efficiency and usability. We now argue that the user does *not* need to choose the values of n if we appeal to the convexity of the (θ_1, θ_2) -space such that $\theta = h(\theta_1, \theta_2) \in (\delta_1, \delta_2)$ when $\theta = \theta_1 - \theta_2$ or $\theta = \theta_2/\theta_1$. We illustrate that these regions are indeed convex in Appendix C.1 of the supplement.

We note that $(\theta_{1,r}, \theta_{2,r})$ depends on n through the sample size of the joint limiting distribution for $\hat{\boldsymbol{\eta}}_{1,n}$ and $\hat{\boldsymbol{\eta}}_{2,n}$. We now fix the draw \mathbf{u}_r and let the sample size n vary; to make this more clear, we let $\theta_{j,r} = \theta_{j,r}^{(n)}$. For a given draw \mathbf{u}_r , $(\hat{\boldsymbol{\eta}}_{1,n}(\mathbf{u}_r), \hat{\boldsymbol{\eta}}_{2,n}(\mathbf{u}_r))$ will be closer to $(\boldsymbol{\eta}_{1,0}, \boldsymbol{\eta}_{2,0})$ for larger values of n by properties of conditional multivariate normal distributions. Although not guaranteed, $(\theta_{1,r}^{(n)}, \theta_{2,r}^{(n)})$ should also generally be closer to $(\theta_{1,0}, \theta_{2,0})$ for larger values of n . It follows that for larger values of n , (i) the mean of the $N(\boldsymbol{\theta}_r^{(n)}, I(\boldsymbol{\theta}_r^{(n)})^{-1}/n)$ distribution should generally be closer to $\boldsymbol{\theta}_0$ and (ii) this distribution should generally have smaller variance. We now consider what is likely to occur when $\boldsymbol{\theta}_0 \in (\delta_1, \delta_2)$ and for a given draw \mathbf{u}_r . If $100 \times \gamma\%$ of the $N(\boldsymbol{\theta}_r^{(n_A)}, I(\boldsymbol{\theta}_r^{(n_A)})^{-1}/n_A)$ distribution is contained in the interval (δ_1, δ_2) , then $100 \times \gamma\%$ of the $N(\boldsymbol{\theta}_r^{(n_B)}, I(\boldsymbol{\theta}_r^{(n_B)})^{-1}/n_B)$ distribution should also generally be contained in (δ_1, δ_2) for $n_A < n_B$. In light of this, our method to roughly approximate the power curve generates a single Sobol' sequence of length n_{sob} . We use root finding algorithms (Brent, 1973) to find the smallest sample size n such that $100 \times \gamma\%$ of the $N(\boldsymbol{\theta}_r^{(n)}, I(\boldsymbol{\theta}_r^{(n)})^{-1}/n)$ distribution is contained in the interval (δ_1, δ_2) for $r = 1, \dots, n_{sob}$. We use the empirical CDF of these n_{sob} sample sizes to approximate the power curve.

This approach requires several simplifying assumptions, though only one is not already required by Theorem 1: the convexity of the region such that $\theta \in (\delta_1, \delta_2)$. In situations where the BvM theorem can be appropriately leveraged, we believe that the usability and computational efficiency of this approach to power curve approximation justify its reliance on simplifying assumptions. If we generated samples of various sizes n from $f(y; \boldsymbol{\eta}_{1,0})$ and $f(y; \boldsymbol{\eta}_{2,0})$ to approximate the power curve, we would need to generate substantially more than n_{sob} samples to do so. We recommend using $n_{sob} = 1024$. Moreover, users do not need to choose the sample sizes n to explore when using this approach. In Appendix C.2 of the supplement, we show that this approach gives rise to adequate power curve approximation in situations where the BvM theorem can be reasonably applied.

4.3 An Approach to Estimate the SSSD Using Theorem 1

We now formally describe how to calibrate the target length l for the SSSD with power-based criteria and how to estimate this SSSD using Theorem 1. This approach is detailed in Algorithm 1. We also discuss how to modify the SSSD estimation procedure when users wish to choose values for l and α that are not calibrated with power-based criteria.

Algorithm 1 Procedure to Estimate the SSSD with Power-Calibrated Target Length

```

1: procedure POWERCALIBRATEDSSSD( $\gamma, \Gamma, \delta_1, \delta_2, n_{sob}, f(y; \boldsymbol{\eta}_{1,0}), f(y; \boldsymbol{\eta}_{2,0})$ )
2:   sampSobol  $\leftarrow$  NULL
3:   for  $r$  in  $[1, n_{sob}]$  do
4:     Generate Sobol' sequence draw  $\mathbf{u}_r$ 
5:     Let sampSobol $[r]$  be the smallest sample size  $n$  such that  $100 \times \gamma\%$  of the
        $N(\theta_r^{(n)}, I(\theta_r^{(n)})^{-1}/n)$  distribution is contained in the interval  $(\delta_1, \delta_2)$ 
6:   Let  $\mu_l$  be the  $\Gamma$ -quantile of sampSobol
7:   Let  $\alpha = 1 - \gamma$ 
8:   Use the multivariate delta method to find  $I(\theta_0)^{-1}$ 
9:   Let  $l = 2z_{1-\alpha/2}I(\theta_0)^{-1/2}/\sqrt{\mu_l}$ 
10:  Let  $A^2$  be the variance of the limiting distribution for  $\sqrt{n}(I(\hat{\theta}_n)^{-1/2} - I(\theta_0)^{-1/2})$ 
11:  Let  $\sigma_l = 4z_{1-\alpha/2}A/l$ 
12:  return  $\mu_l$  and  $\sigma_l$ 

```

Lines 2 to 5 of Algorithm 1 summarize the process to roughly approximate the power curve developed in Section 4.2. This subprocess returns a vector of sample sizes **sampSobol**. Line 6 shows that we calibrate the length criterion with the target power Γ by choosing μ_l to be the Γ -quantile of **sampSobol**. In Line 7, we choose the coverage $1 - \alpha$ of the posterior HDI to coincide with the conviction threshold γ . Line 8 notes that we must compute $I(\theta_0)^{-1}$ as detailed in Section 4.2. Line 9 rearranges the formula in (7) to select a target length l that will yield the desired value of μ_l for fixed HDI coverage $1 - \alpha$. This calibrates the length criterion and power criterion when $\mathbf{Y}^{(n)} \sim p(\mathbf{y}^{(n)})$. The median of the SSSD is a sample size n such that (i) the posterior HDI for θ has expected length of l and (ii) we expect that $CPM \geq \gamma$ with probability Γ .

If one wants to use alternative values for l and α , they could skip Lines 2 to 7 of Algorithm 1. In Line 9, they would return $\mu_l = 4z_{1-\alpha/2}^2 I(\theta_0)^{-1}/l^2$ as in (7). This is the only modification in this case. To estimate σ_l as described in Section 3.3, we must first find A^2 , the variance of the limiting distribution for $\sqrt{n}(I(\hat{\theta}_n)^{-1/2} - I(\theta_0)^{-1/2})$ as outlined in Line 10. The multivariate delta method can again be used to find this approximately normal distribution: $\sqrt{n}(I(\hat{\theta}_n)^{-1/2} - I(\theta_0)^{-1/2})$ is also a function of $\hat{\boldsymbol{\eta}}_{1,n}$ and $\hat{\boldsymbol{\eta}}_{2,n}$. To implement the multivariate delta method, numerical methods (Gilbert and Varadhan, 2016) can be used to compute the partial derivatives of $I(\theta_0)^{-1/2}$ with respect to $\boldsymbol{\eta}_{1,0}$ and $\boldsymbol{\eta}_{2,0}$. Given A^2 , we estimate σ_l as detailed in Line 11.

4.4 Practical Considerations

In this subsection, we discuss practical considerations for SSSD estimation using Algorithm 1. To use Algorithm 1, we must choose a parametric statistical model for both groups, characteristics θ_1 and θ_2 , an interval (δ_1, δ_2) , a conviction threshold γ , a target power Γ , and design values $\boldsymbol{\eta}_{1,0}$ and $\boldsymbol{\eta}_{2,0}$. In general, we recommend using visualization techniques to help choose the design values. The existing literature on prior elicitation could be of use when specifying the design distributions (Winkler, 1967; Chaloner, 1996; Johnson et al., 2010).

We now illustrate how to implement Algorithm 1 for the example from Section 2.2. For this example, we chose δ_* to be 0.1, so $\delta_1 = \delta_2^{-1} = 1.1^{-1}$. We also specify a conviction threshold of $\gamma = 0.9$ and a target power of $\Gamma = 0.8$. Because the ENIGH survey is conducted biennially, we choose design values for both gamma distributions using data from the ENIGH 2018 survey (INEGI, 2019). We repeat the process detailed in Section 2.2 to create a similar data set of 2018 quarterly food expenditure per person. We adjust each expenditure to account for inflation, compounding 2% annually, between 2018 and 2020. We then find the posterior means for the shape and rate parameters of each gamma distribution using the SIR algorithm as in Section 2.2. These posterior means are $\tilde{\alpha}_1 = 2.43$ and $\tilde{\beta}_1 = 0.79$ for the male provider group and $\tilde{\alpha}_2 = 2.11$ and $\tilde{\beta}_2 = 0.69$ for the female provider group. These posterior means comprise the design values $\boldsymbol{\eta}_{1,0}$ and $\boldsymbol{\eta}_{2,0}$. After accounting for inflation, the 2018 estimate for the median quarterly food expenditure per person in upper income households is 4.29 (MXN \$1000). For the purposes of sample size determination, we use $\kappa_0 = 4.29$ as the threshold for the gamma tail probabilities.

When using a 4-dimensional Sobol' sequence of length $n_{sob} = 1024$, we estimate the 0.8-quantile of the power curve to be 3588.30, which becomes our power-calibrated value for μ_l . We let $\alpha = 1 - \gamma = 0.1$. These values for μ_l and α return a target length of $l = 0.1185 < \delta_2 - \delta_1 = 0.1909$. Finally, Algorithm 1 returns a σ_l value of 269.71. If we were to choose a sample size of $n = \mu_l = 3588.30$, we would expect our Bayesian equivalence test to have power of roughly 0.8 and the 90% posterior HDI for θ_2/θ_1 to satisfy the length criterion ($l = 0.1185$) with probability of roughly 0.5. If we selected a sample size greater (less) than $\mu_l = 3588.30$, then we would expect both the power criterion and length criterion to be satisfied more (less) often.

Neither this SSSD nor this estimated power curve account for the prior distributions. We discuss a simulation-based approach to adjust both the SSSD and estimated power curve to reflect prior information in Section 5. The method in Section 5 illustrates that SSSD estimation is useful even when users are *solely* concerned with satisfying power-based criteria; moreover, it demonstrates why it is important to obtain the SSSD $N(\mu_l, \sigma_l^2)$ via Algorithm 1 – not just its mean μ_l . We also discuss how to identify situations where it is important to account for the prior distributions.

Finally, some users may have alternative targets for the length l and coverage $1 - \alpha$ of the posterior HDI.

In these situations, users should consider the probability p with which they want the $100 \times (1 - \alpha)\%$ posterior HDI for $\theta = \theta_1 - \theta_2$ or $\theta = \theta_2/\theta_1$ to satisfy the length criterion. The sample size could then be selected as the $100 \times p^{\text{th}}$ percentile of the SSSD: $\inf\{n \in \mathbb{Z}_+ : \Phi(\sigma_l^{-1}(n - \mu_l)) \geq p\}$.

5 Accounting for the Prior Distributions

5.1 Motivation

Algorithm 1 can be soundly used when the sample sizes $\{n \mid n \in (\mu_l \pm 3\sigma_l)\}$ are large enough to ensure the data blunts the impact of prior information on the posterior of θ . We discuss how to identify these situations in Section 5.2. However, there may be situations where we would prefer to use priors for Bayesian equivalence tests that are informative relative to the sample size. In Section 5.3, we introduce a simulation-based method for estimating the SSSD that accounts for such prior distributions. This method for SSSD estimation also yields a local approximation to the power curve that incorporates prior information. This method is much faster than traditional simulation-based methods for power curve approximation, but it is slower than the approach from Section 4. Thus, if one is using uninformative priors or anticipates collecting a lot of data, the method proposed in Section 4 is preferred.

This approach also assumes that the SSSD is approximately normal, which is a reasonable assumption because we still require that the conditions for Theorem 1 are satisfied. The simulation-based method, however, relaxes the requirement that the posterior distribution of θ is approximately $N(\theta_0, I(\theta_0)^{-1}/n)$. This is useful when the sample size n is large enough to ensure the posterior of θ is approximately normal but not large enough to guarantee this distribution has mean and variance of roughly θ_0 and $I(\theta_0)^{-1}/n$, respectively. When this occurs for large enough sample sizes n , this means that the impact of prior information on the posterior of θ is material and should be accounted for when choosing sample sizes. We explore the performance of this approach via simulation in Section 6.1.

5.2 Fast Approximation of Expected HDI Length

Here, we discuss a method to quickly estimate $\mathbb{E}(L_{1-\alpha}(\mathbf{Y}^{(n)}))$ for a sample size n . We first generate a non-random, representative sample from $f(y; \boldsymbol{\eta}_{1,0})$ and $f(y; \boldsymbol{\eta}_{2,0})$ as follows. We split the unit interval into $\lceil n \rceil$ equally sized sections. We use the midpoint from each section to generate an observation from each group of design data using CDF inversion. Thus, the empirical CDF of this sample from each group is similar to the CDF of its design distribution.

We then use the SIR algorithm with the following proposal distribution $c_j(\cdot)$ for groups $j = 1$ and 2 : $N(\boldsymbol{\eta}_{j,0}, 1.5 \times I^{-1}(\boldsymbol{\eta}_{j,0})/n_j)$. Because our sample has been chosen non-randomly to coincide with the design distributions, the normal proposal distributions are parameterized by $\boldsymbol{\eta}_{j,0}$ instead of $\hat{\boldsymbol{\eta}}_{j,n_j}$ as in Sections 2.2 and 4.4. By the BvM theorem, these proposal distributions should perform well when the

relevant prior distributions are uninformative or well specified with respect to the design distributions. If one wishes to counterintuitively specify prior distributions that do not coincide with the design distributions, we recommend using MCMC instead of the SIR algorithm. We then use the functions $g(\cdot)$ and $h(\cdot)$ to transform these observations from the posteriors of $\boldsymbol{\eta}_1$ and $\boldsymbol{\eta}_2$ into an approximate sample from the posterior of θ (that is based on the analysis priors). For this posterior, we then calculate the length of the $100 \times (1 - \alpha)\%$ HDI, which serves as a rough estimate for $\mathbb{E}(L_{1-\alpha}(\mathbf{Y}^{(n)}))$.

We comment on why this rough estimate for $\mathbb{E}(L_{1-\alpha}(\mathbf{Y}^{(n)}))$ is suitable. For a particular analysis prior and sample size n , the length of the $100 \times (1 - \alpha)\%$ HDI depends on $\mathbf{Y}^{(n)}$, which we assume is generated by the design distributions. The data can be summarized by the MLEs $\hat{\boldsymbol{\eta}}_{1,n}$ and $\hat{\boldsymbol{\eta}}_{2,n}$. For large sample sizes n , these MLEs are approximately jointly normally distributed in a neighbourhood of $(\boldsymbol{\eta}_{1,0}, \boldsymbol{\eta}_{2,0})$. The size of this neighbourhood around $(\boldsymbol{\eta}_{1,0}, \boldsymbol{\eta}_{2,0})$ decreases as n increases. In general, $L_{1-\alpha}(\hat{\boldsymbol{\eta}}_{1,n}, \hat{\boldsymbol{\eta}}_{2,n}) : \mathbb{R}^{2d} \rightarrow \mathbb{R}^+$ is not a linear function, but its linear approximation is often serviceable near $(\boldsymbol{\eta}_{1,0}, \boldsymbol{\eta}_{2,0})$. Because of this approximate linearity and the symmetry of the limiting multivariate normal distribution for $(\hat{\boldsymbol{\eta}}_{1,n}, \hat{\boldsymbol{\eta}}_{2,n})$, the length of the $100 \times (1 - \alpha)\%$ HDI at $(\hat{\boldsymbol{\eta}}_{1,n}, \hat{\boldsymbol{\eta}}_{2,n}) = (\boldsymbol{\eta}_{1,0}, \boldsymbol{\eta}_{2,0})$ should provide a *rough* approximation of $\mathbb{E}(L_{1-\alpha}(\mathbf{Y}^{(n)}))$. This approximation method is incorporated into our simulation-based approach to SSSD estimation proposed in Section 5.3.

Lastly, we argue that estimating $\mathbb{E}(L_{1-\alpha}(\mathbf{Y}^{(\mu_l)}))$ helps identify situations where we should account for the prior distributions. We let $l^* = \bar{L}_{1-\alpha}(\mathbf{Y}^{(\mu_l)})$ denote our estimate for the expected $100 \times (1 - \alpha)\%$ HDI length for $n = \mu_l$, where μ_l is returned by Algorithm 1. We note that l and l^* should be approximately equal if the sample size $\lceil \mu_l \rceil$ is large enough to blunt the impact of prior information. If l^* is greater than l , this indicates that estimating the SSSD via Algorithm 1 may lead to a smaller probability of satisfying the length criterion than desired. When l^* is (much) smaller than l , this signals that we may not need to collect as much data as suggested by Algorithm 1 to satisfy the length criterion with given probability p . Substantial divergence between l and l^* in either direction suggests that it may be of benefit to estimate the SSSD using the simulation-based approach that incorporates prior information. When comparing the performance of Algorithm 1 and this simulation-based SSSD estimation method in Section 6.1, we include the notion of l^* and demonstrate its value.

5.3 An Approach to Adjust for Prior Information

Stevens and Hagar (2022) proposed a simulation-based method to estimate the SSSD that explores different sample sizes using binary search. This method is prohibitively computationally intensive when conjugate priors are not available. In this subsection, we develop a more efficient simulation-based approach to estimate the SSSD. In particular, the SSSD estimation procedure detailed in Algorithm 2 improves upon the binary search-based approach, with speeds several orders of magnitude faster in certain situations. For the gamma tail probability example from Section 4.4, the simulation-based approach proposed here takes roughly 10

seconds under sufficient parallelization; the SSSD estimation method proposed in [Stevens and Hagar \(2022\)](#) takes about 10 hours using the same computing resources. Our new approach also provides a quick local approximation to the power curve that accounts for the prior distributions.

Algorithm 2 efficiently estimates the SSSD by leveraging theory from univariate probit models. We now show the relationship between the limiting form of the SSSD and the univariate probit model. We suppose the probit model from (8) holds exactly:

$$\Phi^{-1}(Pr(W = 1|N = n)) = \beta_0 + \beta_1 n, \quad (11)$$

where the latent variable for the probit model is given by $\beta_0 + \beta_1 n + \varepsilon$ for $\varepsilon \sim N(0, \sigma_\varepsilon^2)$. Unlike in (9), these error terms are homoscedastic with constant variance σ_ε^2 . The variable N then follows a normal distribution with parameters

$$\mu_N = -\frac{\beta_0}{\beta_1} \quad \text{and} \quad \sigma_N = \frac{\sigma_\varepsilon}{\beta_1}. \quad (12)$$

The SSSD from Algorithm 1 is recovered using (12) when $\beta_0 + \beta_1 n$ is the first-order Taylor approximation to $l - \mathbb{E}(L_{1-\alpha}(\mathbf{Y}^{(n)}))$ at $n = \mu_l$ and when $\sigma_\varepsilon = Var(L_{1-\alpha}(\mathbf{Y}^{(\mu_l)}))$. The slope of the Taylor approximation is

$$\beta_1 = \frac{z_{1-\alpha/2} I(\theta_0)^{-1/2}}{\mu_l^{3/2}}. \quad (13)$$

Together, (12), (13), (7), and $\sigma_\varepsilon = Var(L_{1-\alpha}(\mathbf{Y}^{(\mu_l)}))$ recover $\sigma_l = 4z_{1-\alpha/2}A/l$. A more flexible SSSD estimation approach could allow the components of the probit model (β_0 , β_1 , and σ_ε) to vary from their limiting forms dictated by Theorem 1. Generally, this approach would involve finding $\tilde{\mu}_l$, an estimate for the SSSD mean that incorporates prior information. We could then estimate $Var(L_{1-\alpha}(\mathbf{Y}^{(\tilde{\mu}_l)}))$ to obtain an estimate for σ_ε^2 . Lastly, we could estimate $\mathbb{E}(L_{1-\alpha}(\mathbf{Y}^{(n)}))$ in a neighbourhood of $n = \tilde{\mu}_l$ to find suitable estimates for β_0 and β_1 such that $\beta_0 + \beta_1 n$ approximates $l - \mathbb{E}(L_{1-\alpha}(\mathbf{Y}^{(n)}))$ for sample sizes near $n = \tilde{\mu}_l$. Algorithm 2 details such a procedure.

In Line 2 of Algorithm 2, we implement Algorithm 1 to obtain a target length l and coverage $1 - \alpha$. We also find initial values for μ_l and β_1 via (13). Lines 3 to 6 describe how to get an estimate for μ_l that incorporates prior information. This subprocess involves estimating $\mathbb{E}(L_{1-\alpha}(\mathbf{Y}^{(n)}))$ for two values of n . These quantities should be estimated precisely to minimize the impact of sampling variability. In our numerical studies in Section 6, we averaged 25 estimates for $\mathbb{E}(L_{1-\alpha}(\mathbf{Y}^{(n)}))$ obtained via the SIR algorithm with $v = 450000$ and $\nu = 50000$ each time that we estimated $\mathbb{E}(L_{1-\alpha}(\mathbf{Y}^{(n)}))$. The settings for Algorithm 2 suggested in this subsection are informed by simulations described in Appendix D.1 of the supplement.

Lines 7 to 14 of Algorithm 2 detail a process to efficiently estimate σ_ε . We obtain this estimate via a modified Monte Carlo integration scheme. As in Section 4.2, we obtain a sample of size n_{var} from the joint limiting distribution of $\hat{\boldsymbol{\eta}}_{1,n}$ and $\hat{\boldsymbol{\eta}}_{2,n}$ for $n = \lceil \tilde{\mu}_l \rceil$ using a Sobol' sequence $\mathbf{u}_1, \dots, \mathbf{u}_{n_{var}}$ and conditional multivariate normal distributions. We use $n_{var} = 128$ in our numerical studies. For each Sobol' sequence draw

Algorithm 2 Procedure to Adjust for Prior Information with SSSD Estimation

```

1: procedure PRIORADJUSTEDSSSD( $\gamma, \Gamma, \delta_1, \delta_2, n_{var}, f(y; \boldsymbol{\eta}_{1,0}), f(y; \boldsymbol{\eta}_{2,0})$ )
2:   Obtain  $l, \alpha$ , sampSobol, and initial estimates for  $\mu_l$  and  $\beta_1$  via Algorithm 1
3:   Compute  $l^* = \bar{L}_{1-\alpha}(\mathbf{Y}^{(\mu_l)})$ 
4:   Let  $\dot{\mu}_l$  be  $x$ -intercept of the line with slope  $\beta_1$  that traverses the point  $(\mu_l, l - \bar{L}_{\mu_l})$ .
5:   Compute  $\bar{L}_{1-\alpha}(\mathbf{Y}^{(\dot{\mu}_l)})$ 
6:   Let  $\tilde{\mu}_l$  be the  $x$ -intercept of the line passing through  $(\mu_l, l - \bar{L}_{\mu_l})$  and  $(\dot{\mu}_l, l - \bar{L}_{\dot{\mu}_l})$ 
7:   lenSobol  $\leftarrow$  NULL; pwrSobol  $\leftarrow$  NULL
8:   for  $r$  in  $[1, n_{var}]$  do
9:     Generate Sobol' sequence draw  $\mathbf{u}_r$ 
10:    Generate a non-random sample  $\mathbf{y}^{(n)}$  of size  $n = \lceil \tilde{\mu}_l \rceil$  from  $f(y; \hat{\boldsymbol{\eta}}_{1,n}(\mathbf{u}_r))$  and
       $f(y; \hat{\boldsymbol{\eta}}_{2,n}(\mathbf{u}_r))$  and approximate the posterior
11:    Let lenSobol[ $r$ ] be the estimated length of the  $100 \times (1 - \alpha)\%$  posterior HDI
12:    Let pwrSobol[ $r$ ] be  $\mathbb{I}(Pr(\delta_1 < \theta < \delta_2 | \mathbf{y}^{(n)}) \geq \gamma)$ 
13:  Let  $\hat{\sigma}_\varepsilon \leftarrow \text{sd}(\text{lenSobol})$ 
14:  Let  $\hat{\Gamma} \leftarrow \text{mean}(\text{pwrSobol})$ 
15:  Obtain penultimate estimates for the SSSD mean and variance,  $\ddot{\mu}_l$  and  $\ddot{\sigma}_l^2$ 
16:  Estimate  $\mathbb{E}(L_{1-\alpha}(\mathbf{Y}^{(n)}))$  at  $n = \lceil \ddot{\mu}_l - \delta_\mu \rceil$ ,  $\lceil \ddot{\mu}_l \rceil$ , and  $\lceil \ddot{\mu}_l + \delta_\mu \rceil$  for some  $\delta_\mu > 0$ 
17:  Fit a linear model to obtain  $\hat{\beta}_0$  and  $\hat{\beta}_1$ 
18:  Let  $\hat{\mu}_l \leftarrow -\hat{\beta}_0 / \hat{\beta}_1$  and  $\hat{\sigma}_l \leftarrow \hat{\sigma}_\varepsilon / \hat{\beta}_1$ 
19:  Recalibrate the interval-based and power-based criteria using  $\hat{\Gamma}$ 
20:  Let  $\hat{p}$  be the quantile of the SSSD that corresponds (roughly) to power  $\Gamma$ 
21:  return  $\hat{\mu}_l, \hat{\sigma}_l, \hat{p}$ , and the approximate power curve

```

\mathbf{u}_r , we follow the process developed in Section 5.2 to generate a non-random sample $\mathbf{y}^{(n)}$ from $f(y; \hat{\boldsymbol{\eta}}_{1,n}(\mathbf{u}_r))$ and $f(y; \hat{\boldsymbol{\eta}}_{2,n}(\mathbf{u}_r))$. During this process, $\hat{\boldsymbol{\eta}}_{1,n}(\mathbf{u}_r)$ and $\hat{\boldsymbol{\eta}}_{2,n}(\mathbf{u}_r)$ are treated as the fixed parameters instead of $\boldsymbol{\eta}_{1,0}$ and $\boldsymbol{\eta}_{2,0}$. We approximate a single posterior for each draw \mathbf{u}_r using the SIR algorithm with larger values of ν (750000) and ν (90000). For each posterior, we estimate the length of its $100 \times (1 - \alpha)\%$ HDI. The standard deviation of these n_{var} lengths provides a rough estimate for σ_ε as illustrated in Line 13. For each approximated posterior, we also record whether the estimate for $Pr(\delta_1 < \theta < \delta_2 | \mathbf{y}^{(n)})$ is greater than the conviction threshold γ . Since we have already approximated these posteriors, we can quickly obtain a rough estimate for the power of the equivalence test at $n = \lceil \tilde{\mu}_l \rceil$ in Line 14, which will be used later.

The last component of the probit model that we must estimate is the linear approximation to $l - \mathbb{E}(L_{1-\alpha}(\mathbf{Y}^{(n)}))$ near the SSSD's mean. This process is detailed in Lines 15 to 17 of Algorithm 2. To do so, we compute $\bar{L}_{1-\alpha}(\mathbf{Y}^{(n)})$ for several values near the SSSD mean. We obtain penultimate estimates for μ_l and σ_l to know which sample sizes n to consider. We get these estimates, $\ddot{\mu}_l$ and $\ddot{\sigma}_l$, by using the estimate for σ_ε and the linear equation passing through the points in Line 6: $(\mu_l, l - \bar{L}_{\mu_l})$ and $(\dot{\mu}_l, l - \bar{L}_{\dot{\mu}_l})$. In Line 16, we let δ_μ be such that $\lceil \ddot{\mu}_l - \delta_\mu \rceil$ and $\lceil \ddot{\mu}_l + \delta_\mu \rceil$ correspond to roughly the 45th and 55th percentiles of the $N(\ddot{\mu}_l, \ddot{\sigma}_l^2)$ distribution. For the three values of n listed in Line 16, we compute $\bar{L}_{1-\alpha}(\mathbf{Y}^{(n)})$ using the SIR algorithm with $\nu = 450000$ and $\nu = 50000$ (as in Lines 3 to 6). Here, we average 100 (instead of 25) estimates for $\mathbb{E}(L_{1-\alpha}(\mathbf{Y}^{(n)}))$ to obtain $\bar{L}_{1-\alpha}(\mathbf{Y}^{(n)})$. We use more replications to yield a stable final estimate for σ_l . In Line 17, we fit a linear model to the three $\bar{L}_{1-\alpha}(\mathbf{Y}^{(n)})$ estimates to obtain estimates for the probit

model's slope and intercept: $\hat{\beta}_0$ and $\hat{\beta}_1$. In Line 18, the estimated probit model is used to find $\hat{\mu}_l$ and $\hat{\sigma}_l$, the final estimates for the SSSD's parameters.

We next describe how to recalibrate the interval-based and power-based criteria. This step is mentioned in Line 19 of Algorithm 2. We let $F^*(\cdot)$ be the function obtained via linear interpolation on the empirical CDF of `sampSobol` generated in Algorithm 1. To recalibrate the criteria, we consider the function

$$F^*(p) = F^*(\mu_l + \sigma_l \Phi^{-1}(p)) \quad \text{for } p \in (0, 1),$$

where μ_l and σ_l are returned by Algorithm 1 and $\Phi(\cdot)$ is the CDF of the standard normal distribution. The SSSD from Algorithm 1 has been defined such that $F^*(0.5) = \Gamma$. This definition calibrates the target length and power criterion using asymptotic results. After adjusting the SSSD to account for the prior distributions in Algorithm 2, the median of the SSSD may no longer correspond to the target power Γ . We let $p^* = \Phi(\hat{\sigma}_l^{-1}(\tilde{\mu}_l - \hat{\mu}_l))$. This is the percentile of the $N(\hat{\mu}_l, \hat{\sigma}_l^2)$ distribution at which the estimate $\hat{\Gamma}$ was obtained in Line 14 of Algorithm 2. If the relationship between the two criteria does not need to be recalibrated, then $F^*(p^*)$ should be approximately $\hat{\Gamma}$.

Lastly, we detail how the SSSD yields a local approximation to the power curve near the target power Γ that incorporates prior information. We recalibrate the power curve with the prior-adjusted SSSD using the following function for $p \in (0, 1)$:

$$\hat{F}(p) := \begin{cases} F^*(p) \times \frac{\hat{\Gamma}}{F^*(p^*)} & \text{if } \hat{\Gamma} \leq F^*(p^*) \\ F^*(p) + (1 - F^*(p)) \times \frac{\hat{\Gamma} - F^*(p^*)}{1 - F^*(p^*)} & \text{if } \hat{\Gamma} > F^*(p^*) \end{cases}.$$

$\hat{F}(p)$ makes a proportional adjustment to each value of $F^*(p)$ such that $\hat{F}(p^*) = \hat{\Gamma}$. This adjustment is visualized in Appendix D.2 of the supplement. We define an approximate power curve that incorporates prior information as $(n, \hat{F}(\Phi(\hat{\sigma}_l^{-1}(n - \hat{\mu}_l))))$; this curve passes through the point $(\tilde{\mu}_l, \hat{\Gamma})$. We explore the performance of this fast and rough approximation to the power curve via simulation in Section 6.2. We emphasize that this recalibration procedure and definition of the local approximation to the power curve require that we estimate the entire SSSD $N(\mu_l, \sigma_l^2)$ via Algorithm 1. Therefore, the theoretical results from Theorem 1 are of practical importance – even if practitioners are solely concerned with power-based criteria.

Finally, we let $\hat{p} = \hat{F}^{-1}(\Gamma)$. The $100 \times \hat{p}^{\text{th}}$ percentile of the SSSD returned by Algorithm 2 is the sample size n where the approximate power curve is equal to Γ as mentioned in Line 20. We recommend selecting this value of n as the final sample size. If \hat{p} is close to 0 or 1, this indicates that the initial asymptotic calibration of the target length l and power criterion may not be suitable for the specified prior distributions. We could consider more sophisticated recalibration procedures to address these situations in future work.

6 Numerical Studies

6.1 Comparing SSSD Estimation via Algorithms 1 and 2

We now compare the performance of Algorithms 1 and 2 for estimating the SSSD across several scenarios. For each scenario, we specify the design values and characteristics θ_1 and θ_2 as in Section 4.4 for the gamma tail probability example. These scenarios are based on two sets of prior distributions. For the first set, we specify uninformative GAMMA(2, 0.1) priors for the gamma parameters α_j and β_j for group $j = 1, 2$. To choose the second set of priors, we reconsider the 2018 ENIGH food expenditure data, adjusted for inflation. Using these data and GAMMA(2, 0.1) priors, we obtained posteriors for α_1 , β_1 , α_2 , and β_2 that were approximately gamma distributed in Section 4.4. To discount prior information, we consider gamma distributions that have the same modes with variances that are larger by a factor of 20. In comparison to the GAMMA(2, 0.1) prior, these distributions are quite informative. These distributions – which we use as the set of informative priors – are GAMMA(53.98, 21.74) for α_1 , GAMMA(44.00, 54.09) for β_1 , GAMMA(18.12, 8.15) for α_2 , and GAMMA(14.71, 19.90) for β_2 .

With each prior specification, we consider four $(\gamma, \Gamma, \delta_*)$ combinations: (0.5, 0.6, 0.25), (0.9, 0.6, 0.25), (0.5, 0.8, 0.1), and (0.9, 0.8, 0.1). These combinations have been chosen so that the four values for μ_l differ substantially. These four combinations consider equivalence testing with the PoA, so $\delta_1 = \delta_2^{-1} = ((1 + \delta_*)^{-1})$. For each setting consisting of a prior specification and $(\gamma, \Gamma, \delta_*)$ combination, we consider the performance of both Algorithms 1 and 2 to estimate the SSSD. We consider the performance of Algorithms 1 and 2 for several noninferiority tests in Appendix E of the supplement.

For each setting and algorithm, we generated 100 SSSDs; we then recorded their target lengths and their 5th, 10th, 25th, 50th, 75th, 90th, and 95th percentiles. For each of the 100 estimates of a given percentile, 100 samples of that size were randomly generated from $f(y; \boldsymbol{\eta}_{1,0})$ and $f(y; \boldsymbol{\eta}_{2,0})$. For each sample, the posterior was approximated via the SIR algorithm as in Section 2.2. We then determined whether this posterior HDI satisfied the length criterion corresponding to the SSSD from which the percentile was estimated. Thus, for each percentile, 10000 such classifications were made. We calculated the proportion of the 10000 posteriors whose HDIs satisfy the length criterion. The discreteness of the sample size is inconsequential for larger sample sizes, so roughly $100 \times p\%$ of the posterior HDIs should satisfy the length criterion. The numerical findings for Algorithms 1 and 2 are detailed in Tables 1 and 2 for the settings with uninformative and informative priors, respectively. The $\hat{\mu}_l$ and $\hat{\sigma}_l$ columns denote the sample mean of the 100 generated estimates for μ_l and σ_l . Furthermore, the \hat{l} column denotes the sample mean of the 100 target lengths.

Table 1 shows that Algorithms 1 and 2 generally offer comparable SSSD estimation for the uninformative prior settings. We later discuss the problematic behaviour with the lower SSSD percentiles in setting 1a, corresponding to sample sizes $n < 50$. For the other settings in Table 1, both algorithms produce estimates for μ_l and σ_l such that a sample size informed by the $100 \times p^{\text{th}}$ percentile of this distribution satisfies the

Setting			SSSD Parameters			Proportion with Length Criterion Satisfied						
α	\hat{l}		Alg.	$\hat{\mu}_l$	$\hat{\sigma}_l$	p						
						0.05	0.10	0.25	0.50	0.75	0.90	0.95
1a	0.5	0.316	1	84.90	41.48	0.1244	0.1332	0.2756	0.5269	0.7473	0.8855	0.9345
			2	83.28	46.51	0.2185	0.1218	0.2417	0.5052	0.7544	0.9075	0.9510
1b	0.1	0.347	1	418.65	92.12	0.0424	0.0947	0.2446	0.4934	0.7341	0.8845	0.9385
			2	420.69	94.04	0.0416	0.0934	0.2445	0.5046	0.7515	0.8967	0.9451
1c	0.5	0.098	1	878.33	133.43	0.0513	0.1043	0.2585	0.5099	0.7561	0.8934	0.9451
			2	874.74	136.77	0.0461	0.0885	0.2411	0.5047	0.7572	0.8970	0.9464
1d	0.1	0.119	1	3583.92	269.54	0.0534	0.0990	0.2604	0.4971	0.7625	0.8988	0.9464
			2	3580.69	278.81	0.0504	0.0913	0.2374	0.4989	0.7595	0.9008	0.9430

Table 1: Simulation results comparing the SSSD estimation performance of Algorithms 1 and 2 for the uninformative prior settings

Setting			SSSD Parameters			Proportion with Length Criterion Satisfied						
α	\hat{l}		Alg.	$\hat{\mu}_l$	$\hat{\sigma}_l$	p						
						0.05	0.10	0.25	0.50	0.75	0.90	0.95
2a	0.5	0.316	1	84.91	41.49	0.0618	0.1531	0.3975	0.6983	0.8931	0.9652	0.9855
			2	67.07	38.07	0.0204	0.0687	0.2330	0.5127	0.7590	0.9072	0.9481
2b	0.1	0.347	1	418.30	92.09	0.0599	0.1178	0.3122	0.5899	0.8230	0.9376	0.9682
			2	398.21	88.46	0.0451	0.0895	0.2508	0.5090	0.7482	0.8945	0.9425
2c	0.5	0.098	1	882.19	133.72	0.0619	0.1287	0.3202	0.5866	0.8092	0.9319	0.9676
			2	855.32	130.32	0.0435	0.0976	0.2407	0.4974	0.7450	0.8909	0.9455
2d	0.1	0.119	1	3587.25	269.67	0.0567	0.1153	0.2740	0.5411	0.7790	0.9151	0.9618
			2	3559.25	266.18	0.0484	0.0928	0.2539	0.4956	0.7420	0.8983	0.9392

Table 2: Simulation results comparing the SSSD estimation performance of Algorithms 1 and 2 for the informative prior settings

length criterion with probability approximately p . This suggests that adjusting for prior information is not crucial in these settings. This is supported by the notion of l^* . For each setting, we let \hat{l}^* be the sample mean of the 100 l^* values generated when estimating the SSSD via Algorithm 2. For settings 1b, 1c, and 1d, \hat{l}^* is 0.348, 0.098, and 0.119, respectively. These values are very close to \hat{l} for each of these settings. For setting 1a, $\hat{l}^* = 0.313$, which differs slightly from $\hat{l} = 0.316$.

Table 2 shows that Algorithm 2 performs well except when estimating the lower percentiles of the SSSD in setting 2a. These sample sizes are too small for asymptotic results to be applied. The sample sizes recommended by Algorithm 1 are conservative, particularly for settings 2a, 2b, and 2c. For these settings, \hat{l}^* is respectively 0.286, 0.339, and 0.096; these values are perceptibly less than \hat{l} . Thus, the notion of l^* is useful because we are alerted that we are collecting more data than required to satisfy the length criterion with a given probability p . The performance of Algorithm 1 is somewhat better for setting 2d, for which \hat{l}^* is 0.118; this is a direct result of the BvM theorem. Therefore, it appears that adjusting for prior information might not be necessary if l^* is relatively close to the target length l .

We now discuss the problematic behaviour in setting 1a, where the SSSD is not well defined. For settings 1a and 2a, we generated 10000 samples of size $n = \{1, 2, \dots, 10\} \cup \{15, 20, \dots, 250\}$ from $f(y; \boldsymbol{\eta}_{1,0})$, $f(y; \boldsymbol{\eta}_{2,0})$

and recorded how often the length criterion ($\hat{l} = 0.316$) was satisfied. Figure 2 visualizes these simulation results for settings 1a (left) and 2a (right) along with the SSSDs characterized by $\hat{\mu}_l$ and $\hat{\sigma}_l$ from Tables 1 and 2. For setting 1a, when $n = 1$, the probability of satisfying the length criterion is over 50%! This probability decreases until roughly $n = 20$ and then increases with n .

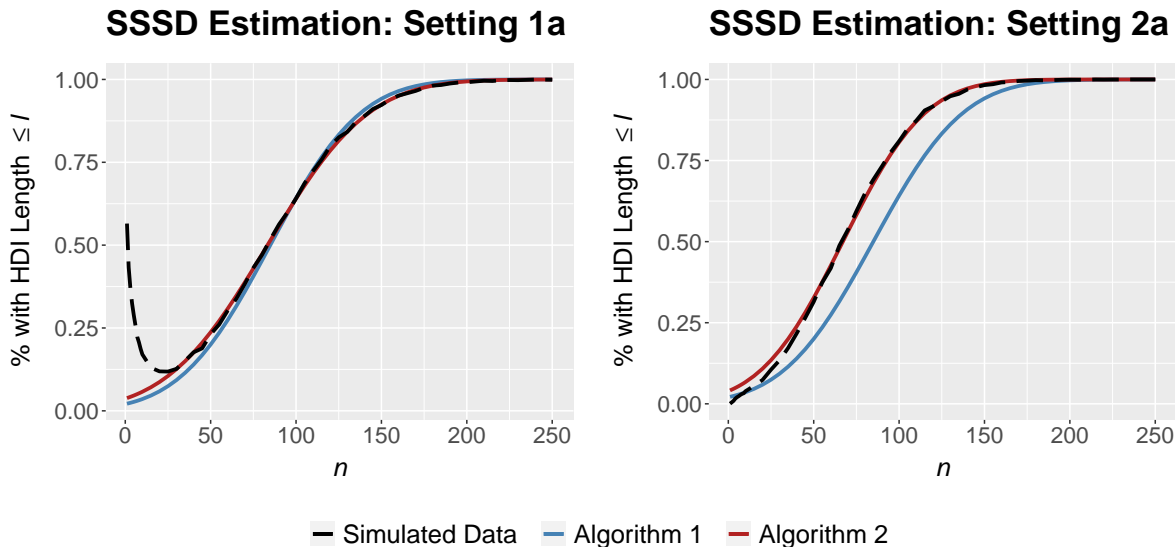


Figure 2: Estimating the probability that the length criterion is satisfied using various methods for settings 1a (left) and 2a (right).

For setting 1a, this explains why Algorithm 2’s entry for the 5th SSSD percentile (0.2185) was greater than the entry for its 10th percentile (0.1218). Most of the 5th SSSD percentiles estimated for setting 1a using Algorithm 2 were less than 10, and most of the 10th SSSD percentiles were between 20 and 30. The right plot in Figure 2 shows that the SSSD is well defined when the informative priors are used. Algorithm 2 does a better job of approximating the trend observed by simulating data. However, the asymptotic results leveraged in Algorithm 2 appear to fail for $n < 40$.

6.2 Evaluating the Local Approximation of the Power Curve

For each setting in Section 6.1, we estimated 100 SSSDs via Algorithm 2. Algorithm 2 also returns a local approximation to the power curve that incorporates prior information. Here, we consider the suitability of this approximation. For each setting, we selected an appropriate array of sample sizes n . For each value of n , we generated 10000 samples of that size from $f(y; \boldsymbol{\eta}_{1,0})$ and $f(y; \boldsymbol{\eta}_{2,0})$. We approximated the corresponding posterior of $\theta = \theta_2/\theta_1$ and determined whether $100 \times \gamma\%$ of the posterior was contained within (δ_1, δ_2) . For each n explored, we computed the proportion of the 10000 samples in which this occurred to approximate the power curve. The results for the settings with uninformative priors (left) and informative priors (right) are depicted in Figure 3.

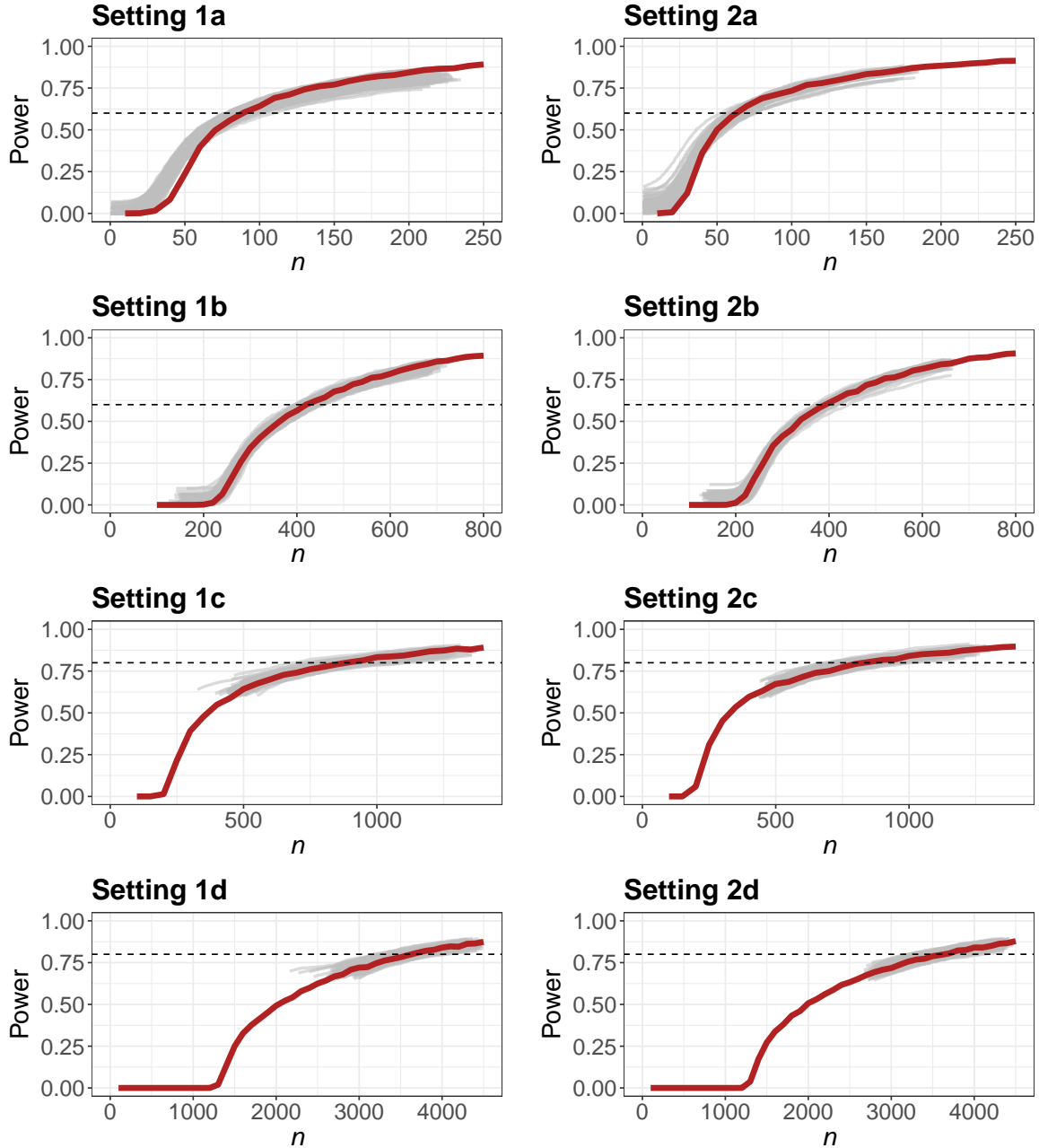


Figure 3: 100 local power curve approximations (semi-opaque grey), power curve estimated via simulated data (red), and target power Γ (dotted line) for each setting.

We first consider the results for the settings with uninformative priors. In general, the power curves provide a good local approximation near the target power Γ . The quality of the approximation appears to deteriorate as we increase or decrease from Γ , particularly for setting 1a as power decreases. For settings 1c and 1d, the local approximation to the power curve does not extend to sample sizes with low power. This occurs because the local approximation leverages the SSSD, which is approximately normal. The power curve typically has a long right tail. Thus, the sample sizes that correspond to low power are virtually the

0th percentile of the power-calibrated SSSD. This yields unstable estimates for power, so we restrict the local approximation of the power curve to the probable domain of the SSSD returned by Algorithm 2. To approximate a different section of the power curve, we could run Algorithm 2 with a smaller Γ value. Most importantly, the approximated power curves generally yield a reasonable sample size recommendation if we want the Bayesian equivalence test to have power of roughly Γ .

We next consider the simulation results for the settings with informative priors. The conclusions are similar to those for the settings with uninformative priors. Once again, the approximate power curves appear to be serviceable near the target power. The adjustment to incorporate prior information is substantial for the settings with smaller sample sizes (2a and 2b), but the approximate power curve reasonably accounts for this.

We reiterate why practitioners would be interested in this method for sample size determination – even if they are not concerned with interval-based criteria. Each of the grey curves in Figure 3 can be estimated in roughly 10 seconds under sufficient parallelization (and in roughly a minute on a laptop with 4 cores). With the same computational resources for this example, we can approximate a *single point* on the power curve using 500 approximated posteriors. This produces a single, crude estimate of power that may not even be close to Γ . Our method for sample size determination allows practitioners to quickly explore potential designs for their study. They can quickly discard unrealistic designs that yield unattainable sample sizes. Even those who prefer the predictive approach might use this method to quickly conduct preliminary exploration of their study design before conducting more computationally intensive simulations.

Finally, this method is not appropriate for small sample sizes. Our method, however, appears to at least inform practitioners when their required sample sizes are small. More traditional simulation-based design methods can be used in these scenarios since they are typically less computationally intensive and easier to implement with small sample sizes.

7 Conclusion

7.1 Discussion

In this paper, we developed a comprehensive framework for sample size determination with Bayesian equivalence tests facilitated via posterior probabilities. This framework is founded on the approximate normality of the SSSD, which we proved under certain conditions. In light of this, we proposed two new methods to estimate this distribution – one that does not account for the prior distributions and another that does at a manageable computational cost. Both approaches are *much* faster than existing methods to estimate the SSSD. We also explored the relationship between interval-based and power-based criteria for Bayesian equivalence tests and incorporated this relationship into our new SSSD estimation approaches. Moreover, the numerical studies conducted show that our methods yield suitable SSSD estimation and local power

curve approximation for large sample sizes.

7.2 Extensions

It may be possible to extend this work to the predictive approach for choosing the sampling distribution of $\mathbf{Y}^{(n)}$. This would prevent us from directly applying the BvM theorem, but perhaps results from the BvM theorem (where we treat a draw from the design prior as the fixed parameter $\boldsymbol{\eta}_{j,0}$) could still be leveraged to yield more computationally efficient sample size recommendations. We could also consider how low-discrepancy sampling techniques might improve the computational efficiency of these sample size determination methods.

Moreover, this framework does not currently support imbalanced two-group sample size determination (i.e., where $n_1 = qn_2$ for some constant $q > 0$). It may be inefficient or impractical to force $q = 1$ when prior information for one group is much more precise, when it is more difficult to sample from one of the groups, or in settings where one treatment is much riskier. Future work could consider extensions to this framework where practitioners specify this constant q . We provide guidance for such an extension in Appendix B.2 of the supplement.

Supplementary Material

These materials include a detailed description of the conditions for Theorem 1, along with additional simulation results and theoretical exposition.

Funding Acknowledgement

This work was supported by the Natural Sciences and Engineering Research Council of Canada (NSERC) by way of CGS M and PGS D scholarships as well as Grant RGPIN-2019-04212.

References

- Adcock, C. (1997). Sample size determination: a review. *Journal of the Royal Statistical Society: Series D (The Statistician)* 46(2), 261–283.
- Anderson-Cook, C. M. and C. M. Borror (2016). The difference between “equivalent” and “not different”. *Quality Engineering* 28(3), 249–262.
- Berry, S. M., B. P. Carlin, J. J. Lee, and P. Muller (2011). *Bayesian adaptive methods for clinical trials*. CRC press.
- Brent, R. P. (1973). An algorithm with guaranteed convergence for finding the minimum of a function of one variable. *Algorithms for Minimization without Derivatives, Prentice-Hall, Englewood Cliffs, NJ*, 61–80.

- Brutti, P., F. De Santis, and S. Gubbiotti (2014). Bayesian-frequentist sample size determination: a game of two priors. *Metron* 72(2), 133–151.
- Chaloner, K. (1996). Elicitation of prior distributions. In *Bayesian biostatistics*, pp. 141–156. Marcel Dekker, New York.
- De Santis, F. (2007). Using historical data for Bayesian sample size determination. *Journal of the Royal Statistical Society: Series A (Statistics in Society)* 170(1), 95–113.
- De Santis, F. and M. P. Pacifico (2004). Two experimental settings in clinical trials: predictive criteria for choosing the sample size in interval estimation. In *Applied Bayesian statistical studies in biology and medicine*, pp. 109–130. Springer.
- Dehaene, S. (2003). The neural basis of the Weber–Fechner law: a logarithmic mental number line. *Trends in Cognitive Sciences* 7(4), 145–147.
- Gilbert, P. and R. Varadhan (2016). numderiv: Accurate numerical derivatives. *R package version 8*(1).
- Gubbiotti, S. and F. De Santis (2011). A bayesian method for the choice of the sample size in equivalence trials. *Australian & New Zealand Journal of Statistics* 53(4), 443–460.
- Hagar, L. and N. T. Stevens (2023). Supplement to “fast sample size determination for Bayesian equivalence tests”. *Bayesian Analysis* (submitted).
- Hofert, M. and C. Lemieux (2020). *qrng: (Randomized) Quasi-Random Number Generators*. R package version 0.0-8.
- Instituto Nacional de Estadística, Geografía e Informática [National Institute of Statistics, Geography, and Informatics] (INEGI) (2019). Encuesta Nacional de Ingresos y Gastos de los Hogares (ENIGH). 2018 Nueva serie [National Survey of Household Income and Expenses. New edition 2018]. www.inegi.org.mx/programas/enigh/nc/2018/#Datos_abiertos.
- Instituto Nacional de Estadística, Geografía e Informática [National Institute of Statistics, Geography, and Informatics] (INEGI) (2021). Encuesta Nacional de Ingresos y Gastos de los Hogares (ENIGH). 2020 Nueva serie [National Survey of Household Income and Expenses. New edition 2020]. www.inegi.org.mx/programas/enigh/nc/2020/#Datos_abiertos.
- Johnson, S. R., G. A. Tomlinson, G. A. Hawker, J. T. Granton, and B. M. Feldman (2010). Methods to elicit beliefs for Bayesian priors: a systematic review. *Journal of clinical epidemiology* 63(4), 355–369.
- Joseph, L. and P. Belisle (1997). Bayesian sample size determination for normal means and differences between normal means. *Journal of the Royal Statistical Society: Series D (The Statistician)* 46(2), 209–226.

- Joseph, L. and D. B. Wolfson (1997). Interval-based versus decision theoretic criteria for the choice of sample size. *Journal of the Royal Statistical Society: Series D (The Statistician)* 46(2), 145–149.
- Kemp, S., M. Grice, D. Makarios, K. Stuart, G. C. Carvell, N. J. Morton, and R. C. Grace (2021). Range and distribution effects on number line placement. *Attention, perception & psychophysics* 83(4), 1673–1683.
- Kruschke, J. K. (2011). Bayesian assessment of null values via parameter estimation and model comparison. *Perspectives on Psychological Science* 6(3), 299–312.
- Kruschke, J. K. (2013). Bayesian estimation supersedes the t test. *Journal of Experimental Psychology: General* 142(2), 573.
- Kruschke, J. K. (2018). Rejecting or accepting parameter values in Bayesian estimation. *Advances in Methods and Practices in Psychological Science* 1(2), 270–280.
- Kruschke, J. K. and T. M. Liddell (2018). The bayesian new statistics: Hypothesis testing, estimation, meta-analysis, and power analysis from a bayesian perspective. *Psychonomic bulletin & review* 25(1), 178–206.
- Lehmann, E. L. and G. Casella (1998). *Theory of point estimation*. Springer Science & Business Media.
- Lemieux, C. (2009). Using quasi-monte carlo in practice. In *Monte Carlo and Quasi-Monte Carlo Sampling*, pp. 1–46. Springer.
- Lindley, D. V. (1997). The choice of sample size. *Journal of the Royal Statistical Society: Series D (The Statistician)* 46(2), 129–138.
- Makowski, D., M. S. Ben-Shachar, S. A. Chen, and D. Lüdtke (2019). Indices of effect existence and significance in the bayesian framework. *Frontiers in psychology* 10, 2767.
- Morey, R. D. and J. N. Rouder (2011). Bayes factor approaches for testing interval null hypotheses. *Psychological methods* 16(4), 406.
- Raiffa, H., R. Schlaifer, et al. (1961). *Applied statistical decision theory*. Boston: Harvard University Graduate School of Business Administration.
- Rubin, D. B. (1987). The calculation of posterior distributions by data augmentation: Comment: A non-iterative sampling/importance resampling alternative to the data augmentation algorithm for creating a few imputations when fractions of missing information are modest: The SIR algorithm. *Journal of the American Statistical Association* 82(398), 543–546.
- Rubin, D. B. (1988). Using the SIR algorithm to simulate posterior distributions. *Bayesian statistics* 3, 395–402.

- Sahu, S. and T. Smith (2006). A bayesian method of sample size determination with practical applications. *Journal of the Royal Statistical Society: Series A (Statistics in Society)* 169(2), 235–253.
- Savage, L. J. (1972). *The foundations of statistics*. Courier Corporation.
- Smith, A. F. and A. E. Gelfand (1992). Bayesian statistics without tears: a sampling–resampling perspective. *The American Statistician* 46(2), 84–88.
- Sobol’, I. M. (1967). On the distribution of points in a cube and the approximate evaluation of integrals. *Zhurnal Vychislitel’noi Matematiki i Matematicheskoi Fiziki* 7(4), 784–802.
- Spiegelhalter, D. J., K. R. Abrams, and J. P. Myles (2004). *Bayesian approaches to clinical trials and health-care evaluation*, Volume 13. John Wiley & Sons.
- Spiegelhalter, D. J., L. S. Freedman, and M. K. Parmar (1994). Bayesian approaches to randomized trials. *Journal of the Royal Statistical Society: Series A (Statistics in Society)* 157(3), 357–387.
- Stevens, N. T. and L. Hagar (2022). Comparative probability metrics: Using posterior probabilities to account for practical equivalence in A/B tests. *The American Statistician* 76(3), 224–237.
- Stevens, N. T., S. E. Rigdon, and C. M. Anderson-Cook (2020). Bayesian probability of agreement for comparing the similarity of response surfaces. *Journal of Quality Technology* 52(1), 67–80.
- Stevens, N. T., S. H. Steiner, and R. J. MacKay (2017). Assessing agreement between two measurement systems: An alternative to the limits of agreement approach. *Statistical Methods in Medical Research* 26(6), 2487–2504.
- van der Vaart, A. W. (1998). *Asymptotic Statistics*. Cambridge Series in Statistical and Probabilistic Mathematics. Cambridge University Press.
- Walker, E. and A. S. Nowacki (2011). Understanding equivalence and noninferiority testing. *Journal of General Internal Medicine* 26(2), 192–196.
- Wang, F. and A. E. Gelfand (2002). A simulation-based approach to bayesian sample size determination for performance under a given model and for separating models. *Statistical Science* 17(2), 193–208.
- Wellek, S. (2010). *Testing Statistical Hypotheses of Equivalence and Noninferiority*. Chapman and Hall/CRC.
- Winkler, R. L. (1967). The assessment of prior distributions in Bayesian analysis. *Journal of the American Statistical Association* 62(319), 776–800.

Supplementary Material for Fast Sample Size Determination for Bayesian Equivalence Tests

A Detailed Description of the Conditions for Theorem 1

A.1 Conditions for the Bernstein-von Mises Theorem

Theorem 1 from the main text requires that the conditions for the Bernstein-von Mises (BvM) theorem are satisfied. These conditions are described in more detail in [van der Vaart \(1998\)](#), starting on page 140. Conditions (B0), (B1), and (B2) concern the likelihood component of the posterior distribution for a parameter θ . (B3) concerns the prior specifications for θ .

- (B0) The observations are drawn independently and identically from a distribution P_{θ_0} for some fixed, nonrandom θ_0 .
- (B1) The parametric statistical model from which the data are generated is differentiable in quadratic mean.
- (B2) There exists a sequence of uniformly consistent tests for testing $H_0 : \theta = \theta_0$ against $H_1 : \|\theta - \theta_0\| \geq \varepsilon$ for every $\varepsilon > 0$.
- (B3) Let the prior distribution for θ be absolutely continuous in a neighbourhood of θ_0 with continuous positive density at θ_0 .

A.2 Conditions for the Asymptotic Normality of the Maximum Likelihood Estimator

Theorem 1 from the main text also requires that the design distributions $f(y; \boldsymbol{\eta}_{1,0})$ and $f(y; \boldsymbol{\eta}_{2,0})$ satisfy the regularity conditions for the asymptotic normality of the maximum likelihood estimator. These conditions are detailed in [Lehmann and Casella \(1998\)](#); they consider a family of probability distributions $\mathcal{P} = \{P_\theta : \theta \in \Omega\}$, where Ω is the parameter space. [Lehmann and Casella \(1998\)](#) use θ as the unknown parameter with true fixed value θ_0 , so we state the conditions using this notation. However, we use $\theta = \theta_1 - \theta_2$ or $\theta = \theta_2/\theta_1$ to compare two characteristics in our framework. For our purposes, the conditions in [Lehmann and Casella \(1998\)](#) must hold for the design distributions (with unknown parameters η_1 and η_2 and true values $\eta_{1,0}$ and $\eta_{2,0}$).

[Lehmann and Casella \(1998\)](#) detail nine conditions that guarantee the asymptotic normality of the maximum likelihood estimator. We provide the following guidance on where to find more information about

these conditions in their text. The first four conditions – (R0), (R1), (R2), and (R3) – are described on pages 443 and 444 of their text. (R4) is mentioned as part of Theorem 3.7 on page 447. (R5), (R6), and (R7) are described in Theorem 2.6 on pages 440 and 441. (R8) is mentioned in Theorem 3.10 on page 449.

(R0) The distributions P_θ of the observations are distinct.

(R1) The distributions P_θ have common support.

(R2) The observations are $\mathbf{X} = (X_1, \dots, X_n)$, where the X_i are identically and independently distributed with probability density function $f(x_i|\theta)$ with respect to a σ -finite measure μ .

(R3) The parameter space Ω contains an open set ω of which the true parameter value θ_0 is an interior point.

(R4) For almost all x , $f(x|\theta)$ is differentiable with respect to θ in ω , with derivative $f'(x|\theta)$.

(R5) For every x in the set $\{x : f(x|\theta) > 0\}$, the density $f(x|\theta)$ is differentiable up to order 3 with respect to θ , and the third derivative is continuous in θ .

(R6) The integral $\int f(x|\theta)d\mu(x)$ can be differentiated three times under the integral sign.

(R7) The Fisher information $I(\theta)$ satisfies $0 < I(\theta) < \infty$.

(R8) For any given $\theta_0 \in \Omega$, there exists a positive number c and a function $M(x)$ (both of which may depend on θ_0) such that $|\partial^3 \log f(x|\theta) / \partial \theta^3| \leq M(x)$ for all $\{x : f(x|\theta) > 0\}$, $\theta_0 - c < \theta < \theta_0 + c$, and $\mathbb{E}[M(X)] < \infty$.

B More Flexible Estimation of the SSSD's Limiting Form

B.1 The Degenerate Case

In Section 3.4 of the main text, we mention several scenarios under which the SSSD may be degenerate. In this subsection, we focus on the case where the SSSD is degenerate for nonzero μ_l . We describe this scenario using a simple example. In this example, we assume that data from group $j = 1, 2$ are generated independently from a Bernoulli model with success probability θ_j . We compare $\theta_1 = \eta_1$ and $\theta_2 = \eta_2$ via their difference. We consider design values $\theta_{1,0} = \theta_{2,0} = 0.5$. These design distributions prompt a degenerate SSSD for all HDI coverages $1 - \alpha$ and target lengths l .

The standard deviation of the SSSD's limiting form dictated by Theorem 1 involves a constant A , which is the square root of the asymptotic variance of $\sqrt{n}(I(\hat{\theta}_n)^{-1/2} - I(\theta_0)^{-1/2})$. We compute A using the multivariate delta method. For this example, this involves taking the derivative of the Fisher information $I(\theta_{j,0})^{-1} = \theta_{j,0}(1 - \theta_{j,0})$ with respect to $\theta_{j,0}$ for groups $j = 1$ and 2 . These derivatives are equal to 0 when $\theta_{j,0} = 0.5$. As a result, both A and σ_l are 0. To compute a prior-adjusted SSSD in Algorithm 2, we require the SSSD returned by Algorithm 1 to be nondegenerate.

In scenarios where the SSSD’s degeneracy is a consequence of A being equal to 0, we can estimate a non-degenerate SSSD as follows. When $A = 0$, we can still estimate μ_l using Algorithm 1 without modifications. In Section 5.3 of the main text, (5.2) shows that σ_l is the quotient of $\sigma_\varepsilon = \text{Var}(L_{1-\alpha}(\mathbf{Y}^{(\mu_l)}))$ and β_1 as defined in (5.3). When $A = 0$, our estimate for σ_ε based on limiting theory that informs σ_l is equal to 0; however, we can compute β_1 as normal. Estimating a nondegenerate SSSD when $A = 0$ therefore requires us to obtain a different estimate for σ_ε . We obtain this estimate by modifying the subprocess used in Lines 7 to 14 of Algorithm 2. For $n = \mu_l$, we use a randomized Sobol’ sequence to obtain draws from the limiting distribution of $\hat{\boldsymbol{\eta}}_{1,n}$ and $\hat{\boldsymbol{\eta}}_{2,n}$: $(\hat{\boldsymbol{\eta}}_{1,n}(\mathbf{u}_r), \hat{\boldsymbol{\eta}}_{2,n}(\mathbf{u}_r)), r = 1, \dots, n_{sob}$. As in Section 4.2 of the main text, we consider the limiting posterior imposed by the BvM theorem, which is $N(\theta_r, I(\theta_r)^{-1}/\mu_l)$ for $r = 1, \dots, n_{sob}$. We compute the $100 \times (1 - \alpha)\%$ HDI length for each of the r limiting posteriors. The sample variance of these r obtained HDI lengths becomes our estimate for σ_ε . This estimate yields a nonzero value for σ_l , which can be used with Algorithm 2.

We note that these estimates for σ_l still tend to be rather small. This implies that the probable domain of the SSSD only corresponds to a small range of power curve quantiles. If adjusting for the prior distributions in Algorithm 2 requires substantial recalibration of the length criterion and target power, then the final recommended sample size will correspond to an extreme percentile of the SSSD. Therefore, such sample size recommendations may be unreliable. As mentioned in Section 5.3 of the main text, we could consider more sophisticated recalibration procedures to address these situations in future work.

B.2 Imbalanced Sample Size Determination

In Section 7.2 of the main text, we acknowledge that this framework does not currently support imbalanced sample size determination (i.e., where $n_1 = qn_2$ for some constant $q > 0$). In this subsection, we provide preliminary guidance to allow for imbalanced sample size determination. This procedure requires practitioners to choose the constant q a priori. Unlike in the previous subsection, this extension requires that we modify both Algorithms 1 and 2.

When $n_1 \neq n_2$, we cannot use Theorem 1 to estimate the limiting form of the SSSD because the multivariate delta method cannot be directly applied to obtain the limiting posterior of θ . Instead, we can use the multivariate delta method find the limiting posterior for each group: $N(\theta_{1,0}, I(\theta_{1,0})^{-1}/n_1)$ and $N(\theta_{2,0}, I(\theta_{2,0})^{-1}/n_2)$. For difference-based comparisons, we can obtain a limiting normal posterior for θ with mean $\theta_{1,0} - \theta_{2,0}$ and variance $I(\theta_{1,0})^{-1}/n_1 + I(\theta_{2,0})^{-1}/n_2$. For ratio-based comparisons, an approximately normal limiting posterior for θ could be found using results from [Díaz-Francis and Rubio \(2013\)](#). We emphasize that these limiting normal posteriors are valid under the assumption that the two groups of data are independent.

To implement Algorithm 1, we approximate the power curve using a randomized Sobol’ sequence as detailed in Lines 2 to 5 of Algorithm 1 in the main text. However, we use the limiting posteriors from the

previous paragraph in Line 5 instead of that obtained by using the multivariate delta method directly. This allows us to find μ_l as detailed in Lines 6 and 7. The next modification involves lines 8 and 9. Here, we take the target length l to be the $100 \times (1 - \alpha)\%$ HDI length of the limiting normal posterior defined for the design distributions $f(y; \boldsymbol{\eta}_{1,0})$ and $f(y; \boldsymbol{\eta}_{2,0})$ and the sample size $n = \mu_l$.

As mentioned in the previous subsection, we can compute σ_l by estimating $\sigma_\varepsilon = \text{Var}(L_{1-\alpha}(\mathbf{Y}^{(\mu_l)}))$ and β_1 as defined in (5.3). We estimate σ_ε using the process detailed in Appendix B.1 with the limiting posteriors from the previous paragraph. We estimate β_1 by taking the $100 \times (1 - \alpha)\%$ HDI length of the limiting normal posterior defined for the design distributions and the sample sizes $n = \mu_l - \delta_\mu$ and $\mu_l + \delta_\mu$. We therefore have estimates for $l - \mathbb{E}(L_{1-\alpha}(\mathbf{Y}^{(n)}))$ corresponding to $n = \{\mu_l - \delta_\mu, \mu_l, \mu_l + \delta_\mu\}$. We estimate β_1 using a linear model and these three points. This yields an estimate for σ_l that defines the limiting form of the SSSD in terms of n_2 . We can use this SSSD to recover the sample size for group 1: $n_1 = qn_2$.

The necessary modifications to Algorithm 2 are minor. To estimate $\mathbb{E}(L_{1-\alpha}(\mathbf{Y}^{(n)}))$ or $\text{Var}(L_{1-\alpha}(\mathbf{Y}^{(\mu_l)}))$ as part of Algorithm 2, we generate non-random, representative samples of size $\lceil n \rceil$ from both groups as described in Section 5.2 of the main text. Here, we generate a sample of that size from group 2. We then round $q\lceil n \rceil$ to the nearest integer and generate a sample of that size from group 1. The remainder of Algorithm 2 can be implemented without modifications.

This framework for imbalanced sample size determination has not been thoroughly explored in numerical studies. Moreover, we may want to consider more sophisticated recalibration procedures with imbalanced sample size determination – particularly if informative priors are used. If these priors have a similar level of informativeness for both groups, prior information may have a more substantial impact on the group with the smaller sample size. As such, we may require more substantial recalibration of the length criterion and target power.

C Additional Material for Fast Approximation of the Power Curve

C.1 Convexity of the ROPE

Our method for fast power curve approximation relies on the convexity of the (θ_1, θ_2) -space such that $\theta = h(\theta_1, \theta_2) \in (\delta_1, \delta_2)$. We illustrate that this convexity holds when $\theta = \theta_1 - \theta_2$ and when $\theta = \theta_2/\theta_1$. Figure C.1 visualizes these regions for difference-based (left) and ratio-based (right) comparisons when $\delta_1 < \delta_2$ are both finite. Moreover, we require that δ_1 and δ_2 are both nonnegative for ratio-based comparisons. These regions are clearly convex. The dotted lines in Figure C.1 denote the vertical and horizontal axes of the plot to show that θ_1 and θ_2 can potentially be negative for difference-based comparisons.

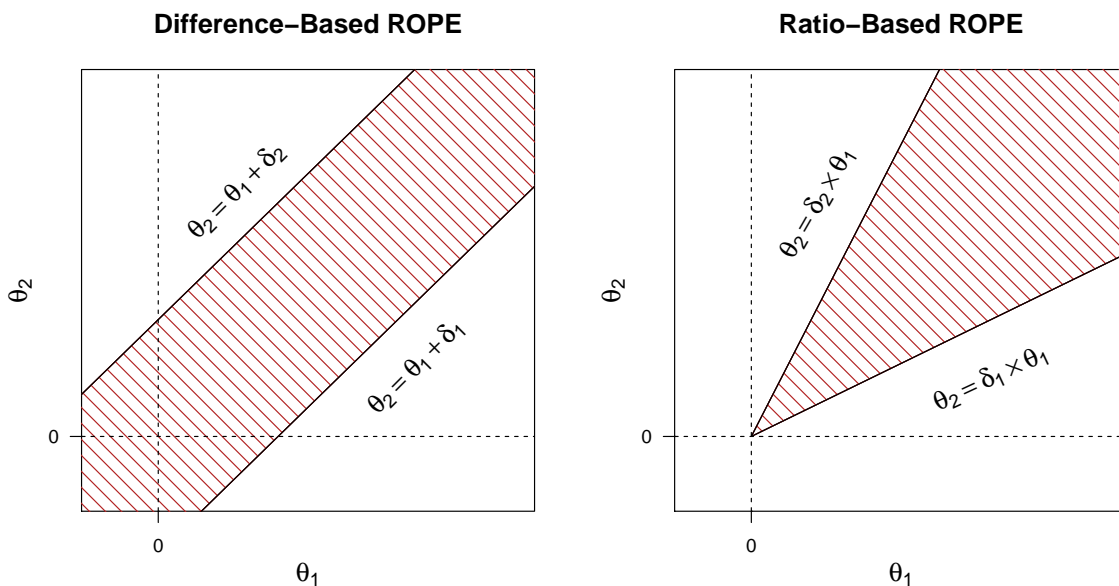


Figure C.1: Visualization of ROPE for difference-based (left) and ratio-based (right) comparisons.

C.2 Simulations to Validate Method

In Section 6.1 of the main text, we generated 100 fast approximations to the power curve using the process detailed in Section 4.2. Please refer to Section 6.1 for more information regarding the scenarios for which these approximate power curves were generated. We argue that these approximations to the power curve are suitable in situations where the BvM theorem can be invoked. The settings with uninformative priors from our simulations (settings 1a, 1b, 1c, and 1d) generally satisfy the conditions to apply the BvM theorem. Moreover, these settings use uninformative priors, so there is not substantial prior information to incorporate. The limiting posterior of θ dictated by the BvM theorem should not differ substantially from the true posterior of θ in these settings.

In Section 6.2 of the main text, we estimated the power curve for each of these settings by simulating data from the relevant design distributions. Per Figure C.2, our method for fast power curve approximation provides excellent approximation for settings 1b, 1c, and 1d. The approximation for setting 1a is not as good as for the other settings. This is particularly true for the smaller sample sizes corresponding to lower power. The method from Section 4.2 assumes that the relevant MLEs are approximately normally distributed. This is not likely to be true for smaller sample sizes. However, our method still provides a suitable rough approximation to the power curve with which to calibrate the length criterion for the SSSD; this power curve approximation is consistent when the asymptotic results hold.

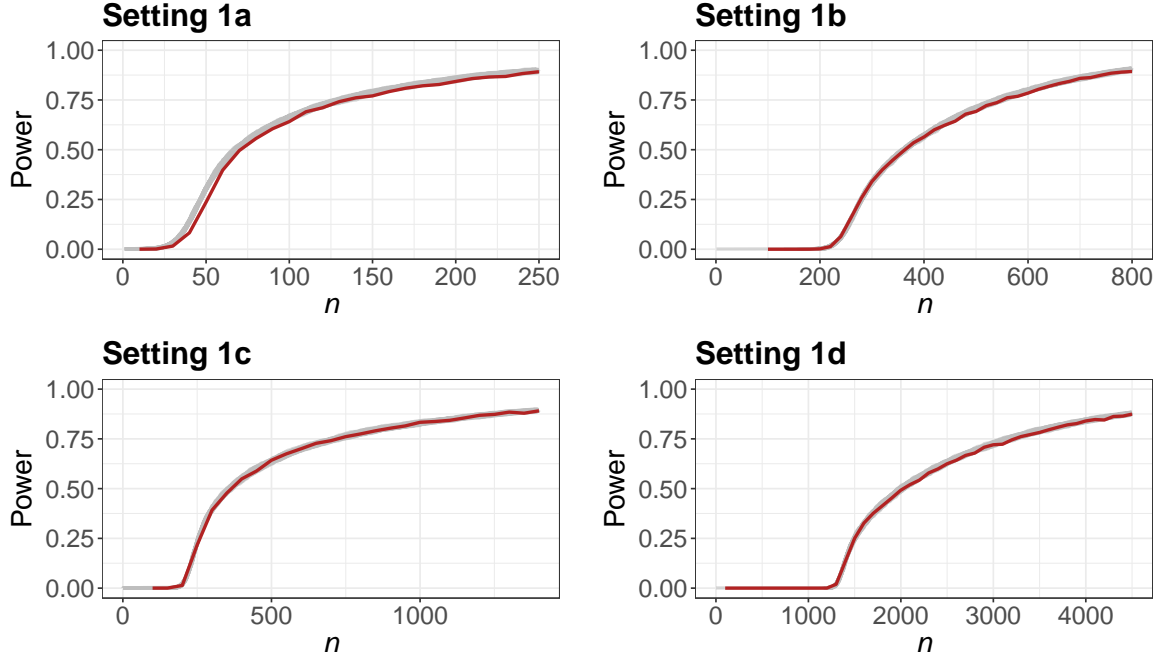


Figure C.2: 100 rough power curve approximations (semi-opaque grey) and power curve estimated via simulated data (red) for each setting with uninformative priors.

D Additional Material for Procedure to Adjust for Prior Information

D.1 Simulations to Justify Settings for Algorithm 2

We used simulation to support the recommendations for the settings used with Algorithm 2 in our numerical studies. For illustration, we considered the SSSD estimation output returned for setting 2b. Please see Section 6.1 of the main text for more background on this setting. We compared the SSSD estimation output from Algorithm 2 with output from the binary search-based algorithm for estimating the SSSD proposed by [Stevens and Hagar \(2022\)](#). Their approach is not a power-calibrated one, so we estimated the SSSD using Algorithm 2 with $\alpha = 0.1$ and $l = 0.347$ instead of implicitly finding a power-calibrated target length. This target length was the mean target length obtained from the numerical studies for setting 2b, as detailed in Table 2 of the main text.

We estimated this SSSD 1000 times using each simulation-based method: the binary-search based approach and Algorithm 2. When using the binary search-based approach, observations are generated directly from the SSSD. [Stevens and Hagar \(2022\)](#) recommend generating 100 observations from the SSSD using this method and estimating the mean and standard deviation of the SSSD using maximum likelihood estimation. We slightly modified the binary search-based approach for use here. [Stevens and Hagar \(2022\)](#) employed Markov chain Monte Carlo (MCMC) methods instead of the SIR algorithm to approximate posteriors corresponding to randomly generated samples from the design distributions. Using MCMC with the binary

search-based approach is prohibitively computationally intensive for the gamma model, a scenario where conjugate priors are not readily available. We therefore instead used the sampling-importance-resampling (SIR) algorithm (Rubin, 1987) as detailed in Sections 2.1 and 2.2 of the main text with $\nu = 10^6$ and $\nu = 10^5$. These SIR algorithm settings were found to yield similar performance to the MCMC settings recommended by Stevens and Hagar (2022) in smaller scale simulations. With Algorithm 2, we used the settings recommended in Section 5.3 of the main text.

Figure D.1 illustrates that using Algorithm 2 with the recommended settings gives rise to much more precise SSSD estimation than using the binary search-based method with 100 SSSD observations. The vertical dotted lines in the Figure D.1 denote the 2.5th and 97.5th percentiles of the 1000 estimated means for the SSSD from each method. These percentiles are much closer together when using Algorithm 2. The horizontal dotted lines denote the 2.5th and 97.5th percentiles of the 1000 estimated standard deviations for the SSSD from each method. For this simulation, these percentiles are again closer together when using Algorithm 2. We repeated this analysis for several settings and obtained similar results each time. Thus,

Comparison of SSSD Estimation: Setting 2b

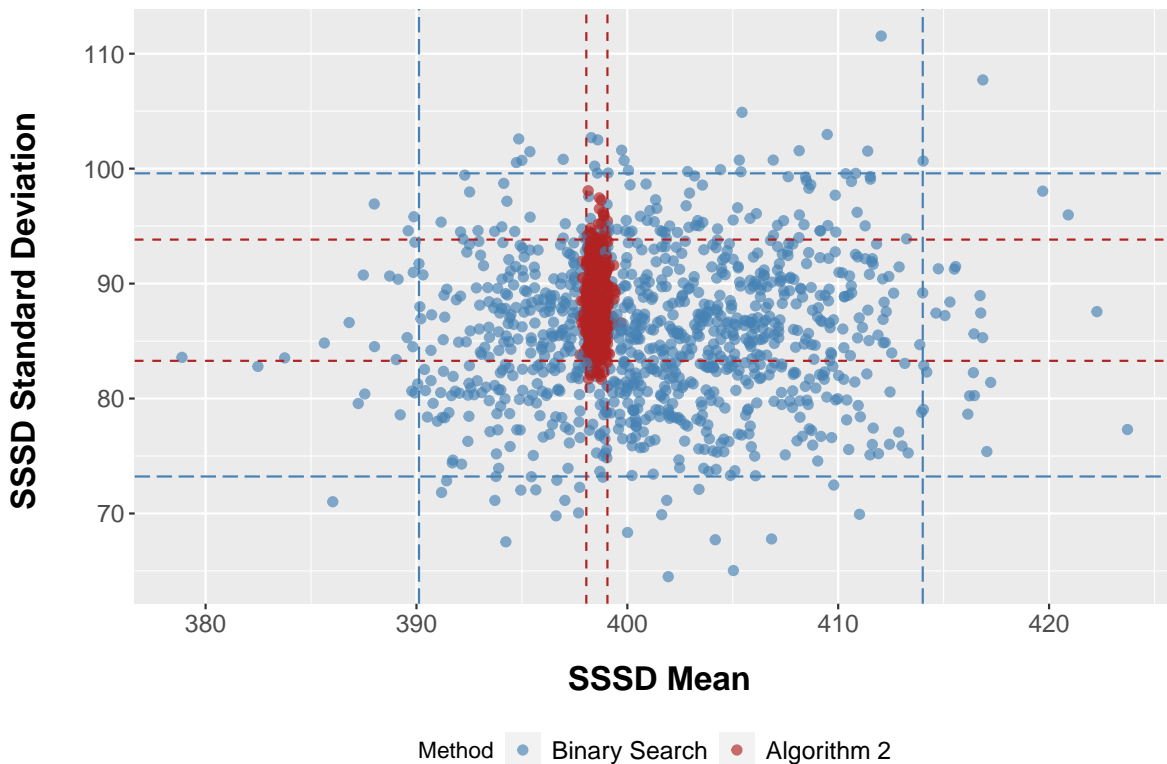


Figure D.1: SSSD estimation comparison for setting 2b from the main text. Vertical dotted lines denote the 2.5th and 97.5th percentiles of the 1000 estimated means for the SSSD from each method. Horizontal dotted lines denote the 2.5th and 97.5th percentiles of the 1000 estimated standard deviations for the SSSD from each method.

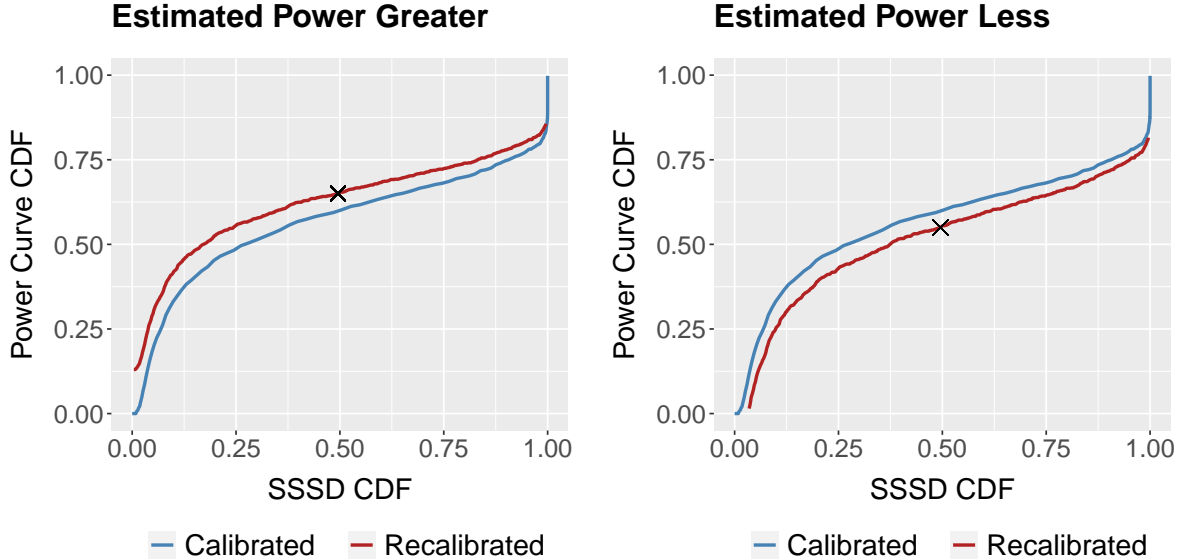


Figure D.2: Example adjustment between the calibration ($F^*(p)$) and recalibration ($\hat{F}(p)$) of the length criterion and target power when $\hat{\Gamma}$ is greater (left) and less (right) than expected. The estimate $\hat{\Gamma}$ is denoted by the “ \times ” in each plot.

using Algorithm 2 with the settings recommended in Section 5.3 of the main text offers more precise (and faster) SSSD estimation than existing methods.

D.2 Visualization of Recalibration Procedure

In Section 5.3 of the main text, we introduced a method to recalibrate the relationship between the interval-based and power-based criteria. This method makes a proportional adjustment to the relationship between the SSSD’s CDF and that of the approximate power curve. Before and after the adjustment, this relationship is respectively characterized by $F^*(p)$ and $\hat{F}(p)$ as defined in Section 5.3 of the main text. Figure D.2 visualizes the proportional adjustment for two example scenarios.

E Numerical Studies with Noninferiority Tests

E.1 Comparing SSSD Estimation via Algorithms 1 and 2

We now compare the performance of Algorithms 1 and 2 for estimating the SSSD with several scenarios corresponding to noninferiority tests. We reuse the settings and prior distributions from Section 6.1 of the main text where $\gamma = 0.9$ (settings 1b, 2b, 1d, and 2d). In this section, we compare θ_1 and θ_2 using the probability of noninferiority (PoNI). The relevant interval for these comparisons is $(\delta_1, \delta_2) = (0, 1 + \delta_*)$ instead of $(\delta_1, \delta_2) = ((1 + \delta_*)^{-1}, 1 + \delta_*)$ as in Section 6.1 of the main text. We do not consider the settings for which $\gamma = 0.5$ because the prior PoNI should be greater than 0.5 if we specify relatively unbiased priors. It is therefore rare to conduct a noninferiority test with a small conviction threshold $\gamma \in [0.5, 1)$. The

Setting			SSSD Parameters			Proportion with Length Criterion Satisfied						
α	\hat{l}		Alg.	$\hat{\mu}_l$	$\hat{\sigma}_l$	p						
						0.05	0.10	0.25	0.50	0.75	0.90	0.95
1b	0.1	0.483	1	216.33	66.22	0.0487	0.0894	0.2362	0.4888	0.7319	0.8868	0.9316
			2	218.68	69.31	0.0418	0.0881	0.2492	0.5051	0.7536	0.8986	0.9493
1d	0.1	0.126	1	3182.54	254.00	0.0486	0.0978	0.2492	0.5021	0.7507	0.8961	0.9472
			2	3180.15	265.96	0.0457	0.0899	0.2298	0.5057	0.7524	0.8968	0.9499

Table E.1: Simulation results comparing the SSSD estimation performance of Algorithms 1 and 2 for the uninformative prior settings

Setting			SSSD Parameters			Proportion with Length Criterion Satisfied						
α	\hat{l}		Alg.	$\hat{\mu}_l$	$\hat{\sigma}_l$	p						
						0.05	0.10	0.25	0.50	0.75	0.90	0.95
2b	0.1	0.483	1	215.84	66.15	0.0592	0.1246	0.3252	0.6163	0.8400	0.9476	0.9734
			2	198.05	62.19	0.0397	0.0878	0.2437	0.4926	0.7559	0.8932	0.9458
2d	0.1	0.126	1	3185.50	254.12	0.0569	0.1175	0.2747	0.5404	0.7795	0.9119	0.9595
			2	3158.47	249.32	0.0505	0.1040	0.2466	0.5091	0.7364	0.8936	0.9459

Table E.2: Simulation results comparing the SSSD estimation performance of Algorithms 1 and 2 for the informative prior settings

numerical study in this subsection is carried out using the same process as described in Section 6.1 of the main text. The numerical findings for Algorithms 1 and 2 are detailed in Tables E.1 and E.2 for the settings with uninformative and informative priors, respectively. These tables are formatted as in Section 6.1 of the main text.

Table E.1 shows that Algorithms 1 and 2 generally produce estimates for μ_l and σ_l such that a sample size informed by the $100 \times p^{\text{th}}$ percentile of this distribution satisfies the length criterion with probability approximately p . This suggests that adjusting for prior information is not crucial in these settings. As in Section 6.1 of the main text, this is supported by the notion of l^* . For each setting, we let \hat{l}^* be the sample mean of the 100 l^* values generated when estimating the SSSD via Algorithm 2. For settings 1b and 1d, \hat{l}^* is 0.485 and 0.126, respectively. These values are very close to \hat{l} for each of these settings. Table E.2 shows that Algorithm 2 performs relatively well. The sample sizes recommended by Algorithm 1 are conservative, particularly for setting 2b. For this setting, \hat{l}^* is 0.463, which perceptibly less than \hat{l} . Thus, the notion of l^* is useful here. The performance of Algorithm 1 is somewhat better for setting 2d, for which \hat{l}^* is 0.125; this is again due to the BvM theorem.

E.2 Evaluating the Local Approximation of the Power Curve

For each setting in Section E.1, we estimated 100 SSSDs via Algorithm 2, which also returns a local approximation to the power curve that incorporates prior information. Here, we consider the suitability of this approximation for noninferiority tests. The numerical study in this subsection is carried out using the same process as described in Section 6.2 of the main text. The results for the settings with uninformative priors (left) and informative priors (right) are depicted in Figure E.1.

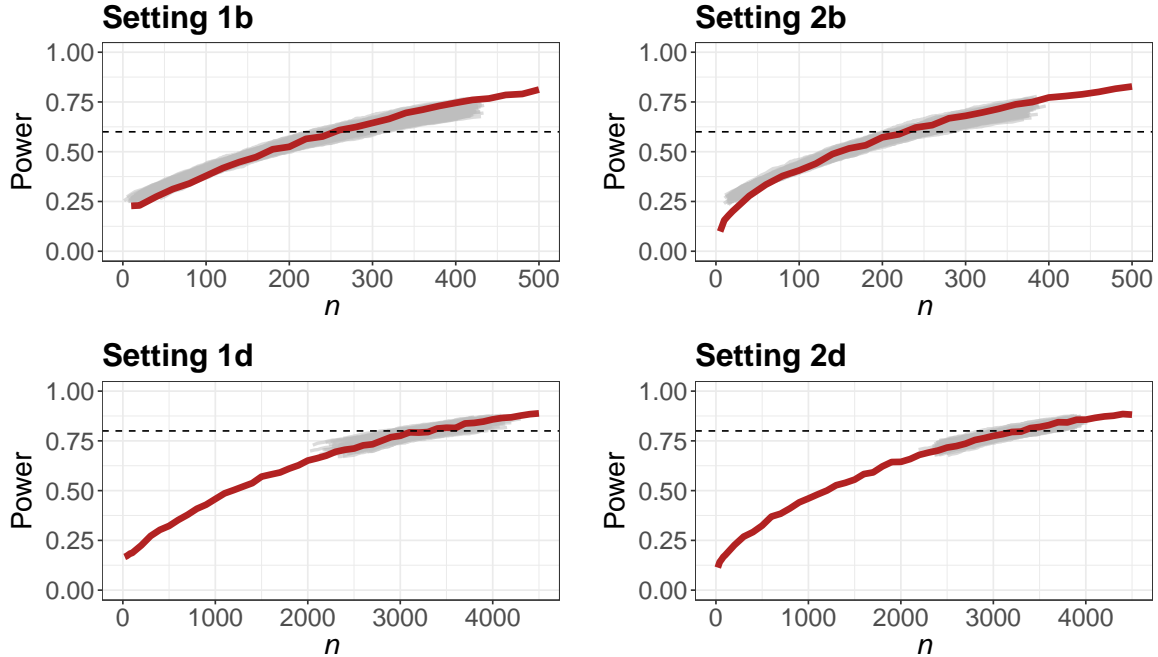


Figure E.1: 100 local power curve approximations (semi-opaque grey), power curve estimated via simulated data (red), and target power Γ (dotted line) for each setting.

We first consider the results for the settings with uninformative priors. In general, the power curves provide a good local approximation near the target power Γ . The quality of the approximation appears to deteriorate as we increase or decrease from Γ , particularly for setting 1b because this setting corresponds to smaller sample sizes. For setting 1d, the local approximation to the power curve does not extend to sample sizes with low power as in Section 6.2 of the main text. We next consider the simulation results for the settings with informative priors. Once again, the approximate power curves appear to be serviceable near Γ . For setting 2b, there is a noticeable deterioration in the power curve approximation for low values of power. The adjustment to incorporate prior information is substantial for setting 2b, but the approximate power curve reasonably accounts for this.

References

- Díaz-Francés, E. and Rubio, F. J. (2013). “On the existence of a normal approximation to the distribution of the ratio of two independent normal random variables.” *Statistical Papers*, 54: 309–323.
- Lehmann, E. L. and Casella, G. (1998). *Theory of point estimation*. Springer Science & Business Media.
- Rubin, D. B. (1987). “The calculation of posterior distributions by data augmentation: Comment: A noniterative sampling/importance resampling alternative to the data augmentation algorithm for creating a few imputations when fractions of missing information are modest: The SIR algorithm.” *Journal of the American Statistical Association*, 82(398): 543–546.

Stevens, N. T. and Hagar, L. (2022). “Comparative Probability Metrics: Using Posterior Probabilities to Account for Practical Equivalence in A/B tests.” *The American Statistician*, 76(3): 224–237.

van der Vaart, A. W. (1998). *Asymptotic Statistics*. Cambridge Series in Statistical and Probabilistic Mathematics. Cambridge University Press.